European
Historical
Economics
Society

EHES WORKING PAPERS IN ECONOMIC HISTORY | NO. 101

You Reap What You Know: Observability of Soil Quality, and Political Fragmentation

Thilo R. Huning
Humboldt-Universität zu Berlin

Fabian Wahl
University of Hohenheim

SEPTEMBER 2016

EHES Working Paper | No. 101 | September 2016

You Reap What You Know: Observability of Soil Quality, and Political Fragmentation*

Thilo R. Huning**
Humboldt-Universität zu Berlin

Fabian Wahl***
University of Hohenheim

Abstract

We provide a theoretical model linking limits to the observability of soil quality to state rulers' ability to tax agricultural output, which leads to a higher political fragmentation. We introduce a spatial measure to quantify state planners' observability in an agricultural society. The model is applied to spatial variation in the 1378 Holy Roman Empire, the area with the highest political fragmentation in European history. We find that differences in the observability of agricultural output explain the size and capacity of states as well as the emergence and longevity of city states. Grid cells with higher observability of agricultural output intersect with a significantly lower number of territories within them. Our results highlight the role of agriculture and geography, for size, political, and economic organization of states. This sheds light on early, though persistent, determinants of industrial development within Germany, and also within Central Europe.

JEL classification: O42, D73, Q15, N93, D82

Keywords: Principal-agent problem, soil quality, urbanization, political fragmentation, Holy Roman Empire

*We would like to thank Sibylle Lehmann-Hasemeyer and Nikolaus Wolf. We would also like to thank Davide Cantoni, Barry Eichengreen, Theocharis Grigoriadis, Erik Hornung, Noel D. Johnson, Peter H. Lindert, Gérard Roland, Stelios Michalopoulos, James A. Robinson, Florentine Schwark, Marvin Suesse, Nico Voigtänder, the participants of the Warwick Economic Growth Summer Workshop, especially Oded Galor, Omer Moav, and Moshe Hazan, the attendants to the seminar in Berlin, and the WEast Workshop in Prague, for their valuable comments. Oliver Salzmann provided excellent research assistance. The usual disclaimer applies.
**Thilo R. Huning is doctoral candidate at the Institute for Economic History, Humboldt-Universität zu Berlin, School of Business and Economics, Spandauer Str. 1, 10997 Berlin, Germany; email: huningth at wiwi.hu-berlin.de.
***Fabian Wahl is post doctoral researcher at the Institute for Economic and Social History with Agricultural History, University of Hohenheim, Wollgrasweg 49, 70599 Stuttgart, Germany; e-mail: fabian.wahl at uni-hohenheim.de

Notice
The material presented in the EHES Working Paper Series is property of the author(s) and should be quoted as such. The views expressed in this Paper are those of the author(s) and do not necessarily represent the views of the EHES or its members

There is a long-standing scholarly debate about the economic determinants of state size and capacity and the origins of territorial states. [1] The determinants of state size are fundamental for understanding the emergence of effective, centralized states. In geographic areas consisting of many states, like Europe during the Middle Ages, barriers to trade and economic exchange are high, as probability of conflicts between various states. Hence, the historically comparatively large amount of small states in Central Europe could account for its relative backwardness during the Middle Ages it could also explain the different points in time at which European regions industrialized.

In this paper we develop a theoretical macroeconomic model that link spatial variation in the size of states within the Holy Roman Empire (HRE) to geographic circumstances. We view state capacity of an agricultural territorial state as an outcome of the combination of the quality, and observability of agricultural output. Our argument is inspired by the study of Mayshar et al. (2014), who develop a principal–agent model of an agricultural state, in which state rulers maximize state revenue, while peasants have incentives to cheat; the peasants ability to do so depends on the quality of the signal, that is, the predictability, or observability, of agricultural output. If output is perfectly predictable, rulers can extract full effort from their peasants, who otherwise have high incentives to swindle their ruler. In a state with a high spatial variation of soil quality, the actual quality of a single plot is hard to observe meaning the ruler will have to estimate the endowment. The lower the observability of soil quality, the lower the state capacity and the smaller the area of a state—as the ruler cannot defend a large territory and is also not able to finance a war to conquer another state. The more heterogeneous, and thus less observable the economy becomes, the higher the costs of observation. Our reasoning is inspired by the fact that, medieval rulers, for example Charlemagne were not only interested in increasing agricultural output, but also in increasing its transparency, uniformity and comparability (Henning, 1994; Hermann, 1985). Due to this, the Charlemagne fostered the introduction of three-field crop rotation . And for the very same reason, buckwheat became increasingly cultivated in the HRE during the 15^{th} century, as it offered safer and less varying yields compared to other, traditional crops (Henning, 1994). Our theoretical argument views state size as endogenously emerging from the rent-seeking activities of autocratic rulers and of conflicts and wars (Spolaore, 2014). The outcome of the rent-seeking considerations as well as the patterns of conflict and war are then in turn determined by the observability of a territory's agricultural output.

Furthermore, the model provides a new explanation for the emergence and survival of historical European city states. City states profited from the lack of powerful neighbors, i.e. they utilized the weakness of territorial states in regions with low agricultural output and observability to gain political independence. They survived and prospered because their economy was not based on agriculture, but on trade and proto-industry. Hence, their ability to tax was decoupled from the quality of the soil. Eventually, proto-industry allowed them to raise much higher revenues. Therefore, they were able to extract enough resources for their defense.

To test our theoretical argument, we propose a measure of observability, based on spatial variation of the suitability of a regions agricultural output, where we measure output with caloric yield. Concretely, we base our measure of observability on the pre-1500 caloric suitability index developed by Galor and Özak (2014, 2015). This index denoted the amount of calories that can be produced

[1] Important studies investigating the determinants of state size and capacity are Alesina and Spolaore (1997); Bolton and Roland (1997); Dincecco (2015); Eisenstadt and Rokkan (1973) and Tilly (1975). Papers concerned with the origins of territorial states are–among others–Ang (2015); Karaman and Pamuk (2011) and Borcan et al. (2014).

in a given area, when the crop with the maximum yield is planted. It is exogenous to human activities and technology (as it does not consider irrigation). Second, it excludes the crops that were not available in Europe, such as potatoes. Third, it reports the maximal caloric yield of all plants cultivable in an area. This accounts for the needs of a society marginally above subsistence, as the index is not distorted by high-value crops. Based on this index we calculate our observability measure as a ruggedness index of caloric yield, i.e. we measure the variation in agricultural output as the variance between the caloric suitability of each cell and that of its neighboring fields. Thus, we capture to what extent the agricultural output of a grid cell diverges from perfect observability (all cells within a grid have the same caloric yield).

The late-medieval HRE was characterized by a historically unique political fragmentation and consisted of territorial, ecclesiastical and city states. This provides an apt setting to test our hypotheses. Furthermore, the political fragmentation peaked in around 1378 when Charles IV. died and we count as many as 716 sovereign territories constituting the HRE at that time.[2] Hence, we focus on the political fragmentation during this period (depicted in Figure 1) as it offers the necessary amount of variation in the size of territories to test our hypothesis empirically.

For the empirical analysis, we split the HRE into grid cells of equal size. We find that grid cells with lower observability of agricultural output are characterized by a significantly higher number of territories. We also show that city states emerged primarily in areas with low observability of agricultural output. Our results are robust to a large set of control variables, such as larger grid cell fixed effects, different grid cell sizes, and an alternative measure of agricultural output. Agricultural observability played a crucial role for state size and capacity as well as for the emergence of city states. Our findings support the general notion that geography, climate and agriculture were important factors for long-run development processes (see Diamond (1999), and Olsson and Hibbs (2005)), and and give empirical support for the theoretical outline by Mayshar et al. (2014).

We make several contributions to the literature. First, our study adds to existing empirical research about the origins and development of states and state capacity in Europe. The existing literature is almost exclusively concerned with the rise of effective states in Europe after the Thirty Years War (Dincecco, 2015) or with the origins and persistence of statehood itself (Ang, 2015; Bockstette et al., 2002; Borcan et al., 2014). There are only two empirical studies that are directly concerned with the origins and evolution of states in pre-modern Europe. The first study is Abramson (2016) who concludes that the revival of urban commerce during the late medieval period was the main cause of the persistently high political fragmentation. Thus, he confirms the older argument of Tilly (1975) that the rise of city states and the urban economy were responsible for the high political fragmentation in Europe. The second study, Ko et al. (2014) ascribes the different historical levels of political fragmentation in Europe and China to the various threats of nomadic invasions faced by both parts of the world.[3]

[2]This number only includes territories north of today's Italy that are included in the map of B.1. If one would also include the Italian territories the number would be even larger.

[3]Another, relevant study is Kitamura and Lagerlöf (2015) who investigate the determinants of historical and contemporary borders in Europe during the period 1500–2000. They found that in general, geographic features (rivers, mountains, coastlines) are important determinants of border locations, although their importance declined over time—with the exception of mountains becoming more important over time. They also find that areas with irrigated agriculture–where rulers control water supply–show less borders. Finally, they show that geography cannot fully account for the political fragmentation in Europe. Their findings thus suggest, that there must be some other overlooked factors that are crucial for the explanation of political fragmentation.

Second, as we explore the origins of historical European city states we complement the findings of existing studies on the roots of the European urban network (Bosker et al., 2013; Bosker and Buringh, 2016). This literature highlighted the importance of preferential location for water- and land-based transport (i.e., a location along rivers, coasts and Roman roads). However, there is also evidence for the importance of second-nature geography, i.e. a city's relative position in the urban network (market potential) and the existence of an "urban shadow effect" meaning that cities prevented the development of other large cities nearby. We show that our observability of agricultural output was decisive for the emergence of city states. Hence, we underline the importance of biogeography and agriculture for the rise of urban Europe and for the understanding of differences in political institutions (Bentzen et al., 2016).

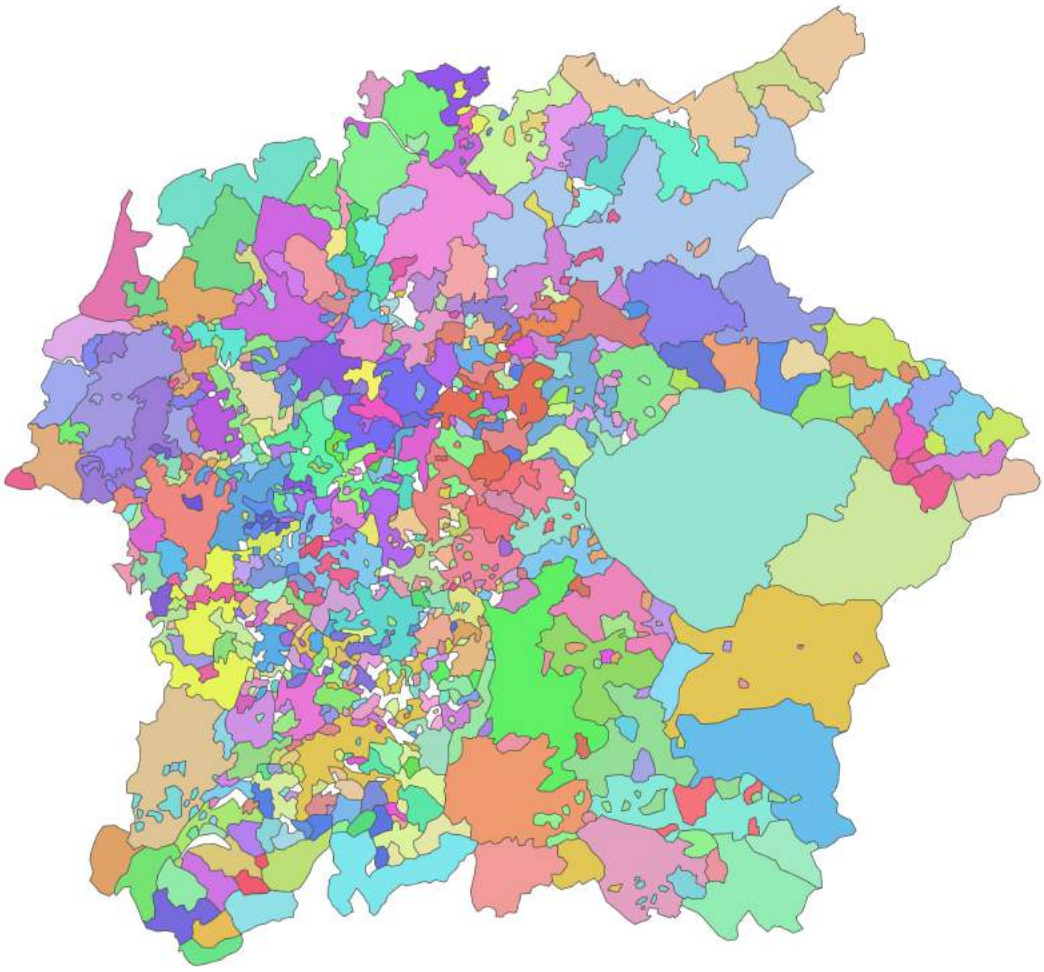

Note: This figure shows territories of the HRE in 1378.

Figure 1: *Digitized map of the German lands 1378 after Wolff (1877).*

Third, we aim to understand the origins of the historical political fragmentation of Central Europe,

which is highly relevant for the understanding of the institutional legacy of Central Europe. In doing so, we contribute to an ongoing debate about whether political fragmentation is harmful or advantageous for long-run development. Many scholars, especially German-speaking historians like Wehler (1995), connect the high degree of centralization of both England and France to the Glorious and 1789 revolutions, which turned both states into liberal, and parliamentary states, whereas the HRE, fragmented and thus lacking the critical mass for violent revolution, blocked the emergence of democratic institutions, and ultimately prepared the grounds for totalitarianism.[4] Furthermore, Acemoglu and Robinson (2006) propose a mechanism for how landed elites could oppose technological progress, and argue that this could in parts account for the relative backwardness of Germany compared to Britain. Aristocratic interests play a vital role in the 1870 shift to grain tariffs significantly slowing down sectoral change (Temin, 2002; Lehmann, 2010). Markets were fragmented until the First World War (Wolf, 2009).The fragmentation of the HRE persists in the form of dialects of the German language, which Lameli et al. (2015) identify as trade barriers to this day.

Fourth, we point out a link between extraction and famine in pre-modern territorial states. In our model, state sizes are limited by the observability of soil, which endogenously limits the occurrence of famines. As stated in Jisheng (2012), Mao Zedong sought to abolish the decentralized and feudalist structures during the 'Great Leap Ahead' as indicated by Marxist ideology. Our model suggests that by doing so, the equilibrium between observability and fragmentation was undermined, and masses of peasants were overtaxed. The outcome was the worst famine in human history.

Emphasizing the advantages of political fragmentation goes back to Montesquieu (1749), and more recently Diamond (1999) and, Hoffman (2015). They argue that the high political fragmentation of Europe fostered political and military innovations and increased investments in state capacity. Wilson (2016) claims that it frustrated censorship, avoided capital–providence tensions, and fostered the "communications revolution"— based on the two German inventions of the printing press and postal service, as the technological reply to a decentralized state. This in turn led to roughly double the amount of publishers per capita compared to France, and to the first daily paper emerging in 1635, 67 years ahead of England. Ko et al. (2014) provide a theoretical model in which the political fragmentation of Europe improved its defensive capacities against external threats (like nomadic invasions), making it more politically stable. Finally, Wilson (2016) argues that the HRE—at least since the Thirty Years War—was a politically stable, comparatively well functioning federation of states Many studies have shown that the pre-modern European city states were comparatively more politically progressive, economically prosperous, and innovative than agriculture-based territorial states (Bosker et al., 2013; Dincecco and Gaetano Onorato, 2016; Stasavage, 2014; Wahl, 2015). Hence, in giving rise to the occurrence of city states, high political fragmentation due to differences in observability of agricultural output could also have contributed positively to the long-run development of the HRE.

In what follows, we will develop a model connecting the principal–agent problem to state capacity, state size and the emergence of city states. We will outline our empirical strategy, in which we

[4]The process of economic integration that preceded political integration was not initiated within the HRE. It took 15 years of Napoleonic Wars, and the Congress of Vienna, to establish the first customs union in history—the German Zollverein—as the economic predecessor of the political unification (Mieck, 1992, p. 193). At Vienna, economic geography and great power politics gave Prussia, less than two decades after it almost disappeared, both motive and means to create a unified nation, and to soon become the largest single market in Europe (Clark, 2007; Huning and Wolf, 2016).

introduce a GIS measure of agricultural observability, and test our theoretical model by grid cell level OLS regressions. We will discuss the results, before concluding.

I. The Evolution of Political Fragmentation in the German Lands from the Carolingian Empire to the Peace Treaty of Westphalia

We will continue with some historical insights to justify three core assumptions of our analysis: First, political fragmentation in the HRE was an outcome of individual state rulers competing for territory and was not centrally planned. Second, we argue that political fragmentation peaked around in 1400 and then continued in a more or less stable equilibrium until the 19th century. Third, we outline the circumstances that sparked the dynamic process we model (around the 10^{th} century), and identify the factors that lead to a replacement of our mechanism (after 1648).

In general, we investigate the evolution of political fragmentation in a medieval and early-modern society which is homogeneous with respect to the agricultural and military technologies used. Furthermore, political power and the capacity of states to make warfare and extract taxes is limited by the same constraints. Thus, the period of our attention begins at the height of the Frankish expansion in 814 when the Frankish Emperor Charlemagne died and ends in the 17^{th} century with the Peace of Westphalia when absolutism and the rise of effective centralized states altered the logic that the size of nations followed. [5]

By c. 800, after more than 300 years of conquest and warfare, the Franks had created the largest political entity in Europe since the fall of the Western Roman Empire. However, the sons of Charlemagne (Charles the Bald, Lothair I, and Louis the German) could not keep the large Empire they had inherited together. Soon after the death of Charlemagne the Carolingian Empire was split among his descendants after a series of military clashes between them.[6] Finally resulting in the Eastern Frankish Empire (which later became the HRE) and the Western Frankish Empire (which eventually became France). However, in East Francia the Carolingian could not maintain their power. During the 10^{th} century, under the rule of the Ottonians, the HRE was formed. The decline of Carolingian weakened the position of the king and the powerful regional dukes filled the vacuumleft by the early death of Emperor Lothair I, leading to the split of his territory, Lotharingia—the central part of the old Frankish Empire, which became part of Eastern Frankish Empire after the treaty of Ribemont.

Additionally, other factors led to a further increase in political fragmentation. One of those important historical events was the vacuum of power created by the break-down of the Staufian dynasty in the 13^{th} century, which resulted in a decade long period without a king (the so called "Great Interregnum").[7]

[5] The following remarks provide a brief and very general sketch of the political history of the Frankish Empire and the HRE until 1378. There are several historical accounts on the European Middle Ages or the medieval history of Germany that offer a much more comprehensive and detailed explanation of the mentioned developments and events. For instance, the reader is referred to Fried (2013) or Heather (2014).

[6] During the 9^{th} century the disputes were settled in the treaties of Verdun (843), Prüm (855), Mersen (870) and Ribemont (880).

[7] For research on what role the Carolingian split-up and the Great Interregnum played for the emergence of city states, and political fragmentation in the HRE, see Jacob (2010) or Stasavage (2011). Another relevant factor was the continuing conflict between the Emperor and the church culminating in the investiture controversy at the end of the 11^{th} century.

Political fragmentation in the successor states of the Eastern Carolingian Empire was high also due to systematic reasons. Central authority was too weak to influence the state rulers' decisions.[8] This was the case, because controlling such a large Empire like the Frankish one posed an enormous challenge at the time. Transport and communication were slow, and so was the flow of information.The development of feudalism and itinerant kingship were the institutional answers of the Carolingians and their successors to those problems. However, compared to France, Feudalism was never as established in the German Lands(Anderson, 1978; Bloch, 1982). As a result of the vacuum of power created by the Carolingian dissolution, the Medieval German Emperors had no large territories that they controlled on their own. In consequence, they were even more dependent on other rulers to provide them with the troops, resources and money necessary for warfare. This absence of a large power base of the Emperors additionally fostered, together with the commercial revolution and the rise of proto-industry, the emergence of prosperous city states and large ecclesiastical territories.

Fragmentation and decentralization of political power peaked in the late Middle Ages. With the Golden Bull of 1356, the election of the king by powerful territorial rulers (the electoral college) made decentralization and political fragmentation officially part of the political structure of the Empire. Consequently, political fragmentation in the HRE peaked in the late 14^{th} century, when in 1378 it consisted of 716 individual territories belonging to 426 sovereign states and remained at this high level until the 17^{th} century.[9]

As a consequence of the Thirty Years' War, many smaller territories lost their independence or were merged with larger states, resulting in a period of political stability within the Empire (Wilson, 2016) During the pre-modern era, organizational and technological innovations changed the nature and costs of warfare and also meant that technological advantages became decisive for military success (Gennaioli and Voth, 2015). Political and societal innovations, overseas trade, and colonialism increased state capacity and tax revenues resulting in a consolidation of political power and the rise of absolutism.[10] The HRE remained relatively politically fragmented until the Napoleonic wars in the early 19^{th} century. However, it was not completely left untouched by these developments as it also increasingly showed centralization tendencies (Wilson, 2016). After the Thirty Years war, the determinants of state capacity and the equilibrium number of states changed fundamentally (Simms, 2013; Wilson, 2009, 2016). As Eugen Weber said, when peasants turned into Germans during the 19^{th} century, the endogenous equilibrium between agricultural observability and size of territories lost its foundation, but left its legacy (Weber, 1976).

We argue that the foundations of political fragmentation lie in variations in the observability of agricultural outputs. As outlined in Mitterauer (2004), the main agricultural innovations of the Middle Ages, the heavy plow and the combination of crop and livestock farming, were available, and applied throughout Central Europe. Deforestation, a necessary prerequisite, had already finished in the 12^{th} century (Wilson, 2016).

[8] External threats to the Carolingian Empire, such as the invasions of the Magyars, Vikings, and the Muslim expansion, put enormous pressure on the successors of Charlemagne. This further weakened their power (Ko et al., 2014).

[9] Ko et al. (2014) and Abramson (2016) both provide figures on the number of states in pre-modern Europe that show the highest number of independent states in around 1400.

[10] Johnson and Koyama (2015) provide a review of the process and determinants of the emergence of centralized and capable states in early-modern Europe.

II. Theoretical Model

The purpose of the theoretical framework is to transfer the insights of the model by Mayshar et al. (2014) to infer variation in sizes of states in the medieval HRE, and also the location of cities. We define a state as an entity that can raise taxes, fight wars against other states, is endowed with soil (a geographic territory), and with labor. We argue that variation in the ability of rulers to tax, caused by variation in the quality of the soil signal (observability), can explain the ability of states to defend themselves, and expand their country. In contrast to Mayshar et al. (2014), we shift the view from a principal-agent perspective to a two-sector output-model. We generalize the two states of nature, high (H) and low (L) from the original model using a continuous measurement of soil quality, for which we will introduce a GIS variable in the empirical part. Our model is static in the agricultural and city sector, and gains its dynamics from the waging of wars.

Assume that states gain income from taxes from agriculture, T^{Λ}, and cities, T^{Ξ}. Having a long-run view on a Malthusian society, population is assumed to be constant. There is a state ruler (principal), and two types of subjects, peasants and citizens (agents). Assume that there is no capital other than soil. State rulers aim to maximize the tax revenue of their state over an infinite time horizon applying a common discount factor δ[11] ,

$$max \left(\sum_{t=0}^{\infty} \left(\frac{T^{\Lambda} + T^{\Xi}}{(1+\delta)^t} \right) \right). \tag{1}$$

I. Agriculture

The theoretical framework outlines the determinants of agricultural production, and links it to spatial variables. This is followed by the outline of the principal-agent problem.

[11] There is an interesting and ongoing debate on between-ruler variation in behavior which would put this in doubt. However, quantitative research hardly finds support for this thesis. For example, Cantoni (2012) rejects the idea that a ruler's age affected its willingness to implement Protestantism.

I.1 Agricultural Output

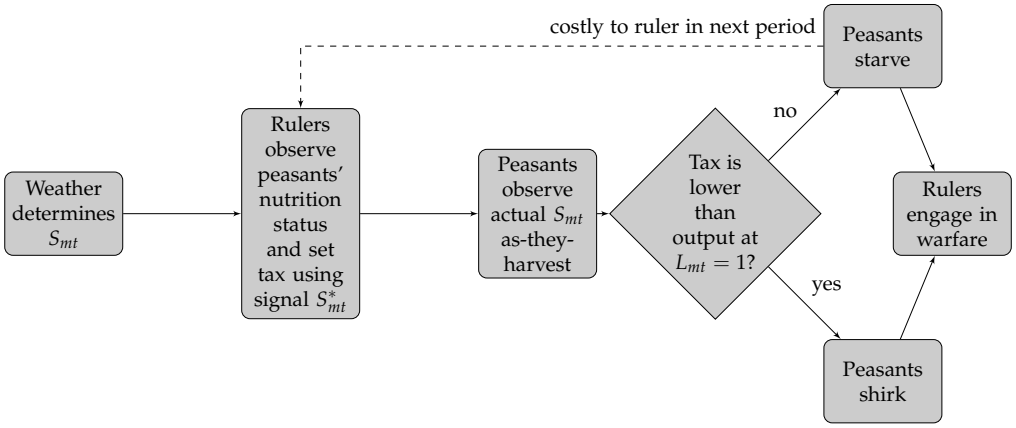

Figure 2: *Graphical representation of seasons in one harvest period as outlined in the formal framework.*

State i splits its area at time t into a set of plots N_{it} and distributes it to peasants to produce agricultural goods. The number of plots is endogenous, and will be explained later. In any harvest period t, production follows a Cobb-Douglas production function with common[12] technology A, constant returns to scale[13], two inputs, labor L and soil S, with substitution elasticity α. Output of any plot m is therefore given by

$$Y_{mt} = AL_{mt}^{\alpha} S_{mt}^{(1-\alpha)} \tag{2}$$

$$S_{mt} = f\left(q_m, \omega_t\right) \tag{3}$$

whereas f is an unobserved functional expression of endowment with factor soil. Function f depends on ω_t, a period fixed and common weather shock[14], and soil quality $q \in [0, \infty)$ measuring the expected value of agricultural output over a long time horizon. To outline the general properties of f, we assume storage technology for inter-temporal transfers exists. There is no soil fatigue, so the quality of the soil is independent of previous harvests, which is a corollary of available technology, and the low degree of intensiveness that agricultural production had compared to modern times. Countermeasures of soil fatigue (most prominently the two-field system and three-field system[15]) were widely applied in the Middle Ages. Investment into soil, e.g. irrigation, is unavailable[16] Thus,

[12]We assume that this technology is the same throughout the HRE. A discussion of technological progress in agriculture in the early Middle Ages is provided by (Mitterauer, 2004, pp. 17). The central claim is that Europe, like the Middle East, experienced an agricultural revolution; however within the HRE, diffusion of technologies was sufficiently fast.

[13]This assumption is not crucial. Assuming the more realistic and also canonical assumption of decreasing returns to scale in the context of a Malthusian society will imply shifts in equilibria, our theorem and corollaries withstanding.

[14]Visualize ω as a vector of many environmental variables, such as exposure to sun, water, rain, humidity, etc.

[15]Our central point is that these technologies disentangled harvests in any year from the harvests of earlier periods. For a discussion of the shift from the two-field system to the three-field-system see (North and Thomas, 1973, p. 43).

[16]As shown in Bentzen et al. (2016), irrigation did not play a role in the HRE except for in some minor regions in Brandenburg. We assume the combination of crop and cattle-farming (see Mitterauer (2004) providing both manure and

$$\frac{\partial f\left(q_m, \omega_t\right)}{\partial q_m} > 0. \tag{4}$$

Assume ω_t is perfectly observable by state rulers and peasants. Its effect for a specific piece of land m is complex, hence not monotonous. Imagine two farms, one on the hill, and one in the valley, and strong rain for days. The hill farmer will find it sufficient to dig some temporary channels to help the excess water find its way downhill; the valley farmer will find his crops flooded. Variation in weather between periods is high, so there is no learning. Despite static variation of output due to weather, its long-run effect is zero[17],

$$\frac{\partial f\left(q_m, \omega_t\right)}{\partial \omega_t} \lessgtr 0 \qquad \lim_{t^* \to \infty} \sum_{t=0}^{t^*} \frac{\partial \, \mathrm{E}(Y_{mt})}{\partial \omega_t} = 0 \tag{5}$$

the higher the standard variation of the signal, $\eta = [0, \infty)$, the less observable is actual land endowment. At $\eta = 0$, both state rulers and peasants can perfectly predict agricultural output. A higher η implies a lower observability. Peasants learn about S_{mt} as they harvest. Mayshar et al. (2014) argue that in the Nile Delta, measuring the extend of flooding was sufficient to estimate agricultural output. The economic intuition is that the marginal effect of water is well-predictable, and in the area where it is, it rises with the degree of flooding in a strictly monotonous fashion. In contrast, in Mesopotamia, measurement was more complex, and thus observability lower. Humans of all ages were well-aware of the different effects of weather on their surroundings, and the degree to which output could be predicted. The signal of soil quality, S^*_{mt}, is normally distributed around actual S_{mt}, so that

$$S^*_{mt} \sim \mathcal{N}\left(S_{mt}, \eta_m\right) \tag{6}$$

I.2 Soil, Effort, and Taxation

State rulers observe the weather, and set the tax just before peasants begin to harvest. For any period t, state rulers wish to extract all output above subsistence s while peasants provide their full labor capacity $L_{mt} = 1$, which we index to one. Thus

$$T_{mt} = A 1^{\alpha} S^*_{mt} \left(q_m, \omega_t, \eta_m\right)^{(1-\alpha)} - s. \tag{7}$$

Consider the case that the state rulers' signal underestimates the possible harvest at full effort by $\epsilon_t^- = (S_{mt} - S^*_{mt}) > 0$. Working on medieval farm comes with risks that are proportional to the effort. Also, state rulers punish any black market interaction. Having to pay more taxes than

animal labor, as a common available technology.

[17] This is tautological in theory as otherwise the effect would be captured by soil quality, but an important prerequisite for empirical analysis.

output (even at full effort), would mean that peasants would starve. To avoid starvation, they are willing to provide labor, although working comes with negative utility,

$$max\left[U\left(L_{mt}, z_{mt}\right)\right] \text{ and } \frac{\partial U}{\partial L} < 0 \text{ but } \frac{\partial U}{\partial L} > \partial\left[-L \mid T_{mt} > Y_{mt}\right] \tag{8}$$

Therefore, peasants will find it optimal to work at full effort if $T_{mt} \geq \left[Y_{mt} \mid L_{mt} = 1\right]$. Else, they will shirk solving for

$$\begin{aligned} A1^{\alpha} {S^*_{mt}}^{(1-\alpha)} &= A\left[L_{mt} \mid S^*_{mt} < S_{mt}\right]^{\alpha} S_{mt}^{(1-\alpha)} \\ A1^{\alpha}\left(S_{mt} - \epsilon_t^-\right)^{(1-\alpha)} &= A\left[L_{mt} \mid S^*_{mt} < S_{mt}\right]^{\alpha} S_{mt}^{(1-\alpha)} \\ \left[L_{mt} \mid S^*_{mt} < S_{mt}\right] &= \sqrt[\alpha]{\frac{1^{\alpha}\left(S_{mt} - \epsilon_t^-\right)^{(1-\alpha)}}{S_{mt}^{(1-\alpha)}}} \end{aligned} \tag{9}$$

From equation 6 and the properties of the normal distribution it follows that the probability of larger ϵ^- increases with a decrease in the quality of the signal η. This means that an underestimation of the soil quality creates a decrease in actual output, in form of a self-fulfilling prophecy.

Consider that state rulers overestimate S_{mt}, so that there exists $\epsilon_t^+ = (S^*_{mt} - S_{mt}) > 0$ The tax would be too high, and the peasants would starve. Assume that taxes relative to subsistence are low, and peasants can starve for one year before dying. State rulers observe starving periods ex post, but before the next harvest. To prevent peasants from dying, and to re-establish full workforce, peasants have to be nursed back to a healthy state $s_h > 1$, which is very costly. Therefore

$$s = \begin{cases} s_0 & \text{if } t = 0 \text{ or } Y_{m(t-1)} = T_{m(t-1)} \\ s_0 + s_h \epsilon_t^+ & \text{else} \end{cases} \tag{10}$$

This means that the output of any harvest period t is path dependent on period $(t-1)$. The dynamic optimization of taxes is retrieved by comparative statics of tax revenue and soil quality and weather,

$$\frac{\partial\left[\sum_{t=0}^{\infty} \frac{\mathrm{E}(T_{mt})}{(1+\delta)^t}\right]}{\partial q_m} > 0 \text{ and } \frac{\partial\left[\sum_{t=0}^{\infty} \frac{\mathrm{E}(T_{mt})}{(1+\delta)^t}\right]}{\partial \sum_{t=0}^{\infty}\left[\omega_t\right]} = 0 \tag{11}$$

Combining the two cases of under- and overestimation for the infinite horizon state rulers regard with discount rate δ, we find that a higher observability of the soil increases expected output. Also, states cannot benefit from a high soil quality if they are not able to observe it. A graphical

representation of the seasons of a harvest period is provided in Figure 2.

I.3 Aggregate Agricultural Output and Allocation of Plots

To close the agricultural sector, state i's total tax from agriculture is derived as the sum over all fields N_{it},

$$T_i^{\Lambda} = \max \left(\sum_{t=0}^{\infty} \frac{\sum_{m \in N_{it}}^{\infty} \mathrm{E}\left(T_{mt}\right)}{(1+\delta)^t} \right) \tag{12}$$

As in Mayshar et al. (2014), state rulers will allocate the plots in their state endogenously. The relationship between the number of plots n and output is convex. If there would be only one plot, state output would be limited by the labor of one peasant, so that $\left[T_i^{\Lambda} \,\middle|\, |N_{it}| = 1 \right] = A1^{\alpha} S_{it}^{*(1-\alpha)}$. In the other extreme case in which the state i allocates too many plots, the land input will be insufficient to yield the expected subsistence of peasants, which is negatively affected by a lower observability due to a larger probability of punishment for starving. The expected tax output $\left[T_i^{\Lambda} \,\middle|\, \lim_{|N_{it}| \to \infty} \right]$ is zero. If land quality would be homogeneous in the whole territory, then the optimal amount of plots $n_{it}^{'} = |N_{it}|$ would be determined by

$$n_{it}^{'} = \underset{n_{it}}{\operatorname{argmax}} \left[n_{it} \left(A1^{\alpha} \left(\frac{\mathrm{E}\left(S_{it}^{*}\left(q_m, \eta_m\right)\right)}{n_{it}} \right)^{(1-\alpha)} - \mathrm{E}(s\left(\eta\right)) \right) \right] \tag{13}$$

This means that the actual allocation of plots will be dependent on the expected output—more suitable territories will have smaller plots, and vice versa. Concerning the observability, larger farms reduce the risk of hunger. Assume that the states are sufficiently large, so that risk diversification is not an issue to state rulers.

Theorem. *The observability of the soil quality determines states' capacity to tax agricultural output*

Proof. See appendix. □

II. Cities

As in Mayshar et al. (2014), states can also allow their subjects to move to cities, in which they will engage in crafts.[18] Crafts follow a Cobb-Douglas production function with technology B and only one input, manual labor, so that any citizen c produces

[18] A discussion on the historical relationship of European urbanization and agricultural productivity is provided by Mitterauer (2002). (Mitterauer, 2004, p. 229) explains how the Mediterranean city states are outliers in their independence of landed aristocracy due to their ability to defend themselves. As this was not given for Central European cities, it is right to assume that state ruler's faced a trade-off between extraction from cities or agriculture.

$$Y_{ct} = BL_{mt} \tag{14}$$

City residents are also subject to taxation. As there is no uncertainty, tax income is perfectly observable. In cities, there is no agriculture.[19] Therefore, food has to be transported to cities at iceberg-type transport cost $\tau > 1$ (assuming agricultural output is perfectly mobile across countries), which increases subsistence costs of the citizens (von Thünen, 1826; Samuelson, 1954). Assume that these costs also allow for grain storage, so that inter-temporal shortages of agricultural production do not affect citizens and the produce from all states taxes can be used to feed citizens. Therefore, citizens never starve and always subsist on s_0, so that

$$T_{ct} = BL_{mt} - \tau s_0 \tag{15}$$

Assume that any state i has z subjects, of which N_{it} are working on fields, then total tax from cities would be given by

$$T^{\Xi} = (z - N_{it}) (BL_{mt} - \tau s_0) . \tag{16}$$

Total tax income T_{it} for any period t would then be given by

$$T_{it} = \sum_{m \in N_{it}}^{\infty} [T_{mt} (A, q_m, \eta_m, s(\eta_m))] + (z - N_{it}) (BL_{mt} - \tau s_0) \tag{17}$$

Proposition 1. *Compared to territorial states, city states show a lower soil quality, or soil observability, or a combination of the two.*

Proof. See appendix. □

III. Warfare

Consider that the states invest all their tax income in the waging of wars with their neighboring states.[20] Assume that any state i is geographically surrounded by a set of countries $J = \{j, j_2, ..\}$. States are perfectly informed about other states tax revenue. Wars take place between harvest periods t and $(t + 1)$. Attacking any plot m comes with fix per-plot costs ψ, and variable costs Δ_m, depending on the budget of the defending state. State i's costs of an attack on plots M_{it} are therefore

[19] As outlined in Allen (2009), the emergence of cities did not depend on spill-overs from agricultural technology, but agricultural technology reacted to demand from cities. We therefore assume for simplicity that any movement of peasants to the city is offset by a technological response.

[20] As assessed in (Mokyr, 2011, p. 392) this would still be true for 17$^{\text{th}}$-century Britain.

$$\mathrm{E}(\Psi_{M_{it}}) = \sum_{m \in M_{it}} [\mathrm{E}(\Delta_m) + \psi] \tag{18}$$

The attack would be successful if the state under attack is not able to bear the costs of Δ_m.[21] Being perfectly informed on T_{it} and T_{jt}, i would only wage the war over m if this is the case, and the war would result in the addition of m to i and a loss to j's territory,

$$m \in \{N_{jt}\},\, m \in \{M_{it}\} \text{ and } \sum_{t=0}^{t^*} T_{it} - \sum_{t=0}^{t^*} \sum_{m \in M_{it}} \Psi_{imt} > \sum_{t=0}^{t^*} T_{jt} - \sum_{t=0}^{t^*} \sum_{m \in M_{jt}} \Psi_{jmt} \Rightarrow$$
$$m \in N_{i(t+1)} \text{ and } m \notin N_{j(t+1)} \tag{19}$$

State rulers are perfectly informed so they observe the present value of any attack on any plot m in period t^*,

$$\sum_{t=t^*}^{\infty} \left[\frac{\mathrm{E}(T_{mt}) - \mathrm{E}(\Delta_{mt}))}{(1+\delta)^t} \right] - \mathrm{E}\left(\frac{\Psi_{m_{it}}}{(1+\delta)^{t^*}} \right). \tag{20}$$

States' cannot borrow[22], so that for any period t^* (expected) state budget of i is given by

$$\forall t^* : \sum_{t=0}^{t^*} \Bigg[\underbrace{\frac{T_{it}}{(1+\delta)^t}}_{\text{Past income}} - \underbrace{\sum_{j \in J} \sum_{n \in N_{it} \cup M_{jt}} \left(\frac{\Delta_{jmt}}{(1+\delta)^t} \right)}_{\text{costs of past defences}} - \underbrace{\sum_{j \in J} \sum_{n \in N_{lt} \cup M_{it}} \left(\frac{\Psi_{jmt}}{(1+\delta)^t} \right)}_{\text{Costs of past attacks}} \Bigg] +$$
$$\underbrace{\sum_{t=t^*}^{\infty} \sum_{m \in N_{it} \cup M_{it^*}} \left(\frac{\mathrm{E}(T_{mt}) - \mathrm{E}(\Delta_{mt}))}{(1+\delta)^t} \right)}_{\text{Expected income}} - \underbrace{\frac{\sum_{t=t^*}^{\infty} \sum_{m \in M_{it}} \mathrm{E}(\Psi_{m_{it}})}{(1+\delta)^t}}_{\text{Expected costs of attacks}} \geq 0. \tag{21}$$

This yields the optimal conquest strategy $P_i = (M_{i1}, M_{i2}, M_{i3}, ...)$, and mutual anticipation induces the expected value of the defense cost to depend on the probability of any m being part of the conquest strategy of a neighbor j_1, so that

[21] A model with dynamic cost of war, featuring endogenous technology and institutions, that can decouple a state from our model, is introduced by Gennaioli and Voth (2015).

[22] This is not a crucial assumption but eases focusing. Relaxing this assumption and installing a present-value borrowing regime (which is not a Ponzi game due to the limits of geography) would lead to the exact same corollaries as the present value of a region converges for defending and attacking state (as risk diversification as a motive is ruled out by assuming reasonably small plots). Under the assumption that default premia are independent of states' capacity to tax, we retrieve the exact same corollaries; assuming that states with lower risks (higher observability) can borrow money cheaper supports our argument.

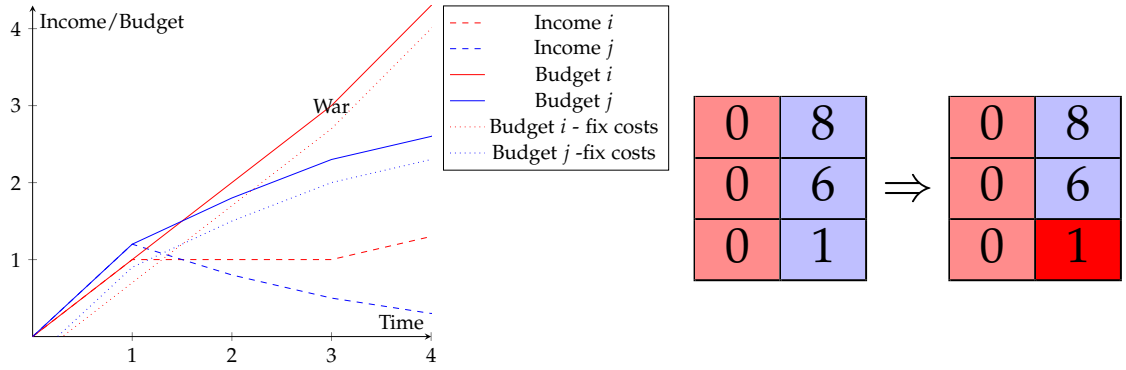

Note: At equal soil quality, state i's aggregated output from agriculture is perfectly observable, while state j's signal is distorted. Therefore i's aggregated income varies significantly between periods, which allows i to pay for the fixed costs of war and overcome j's defense to conquer territory from j after harvest in period 3. State i would do so conditional on the observability of the conquerable plots, and take over the best plots (indicated in dark red). After war, this would cause i to be larger compared to state i. Both states face a decrease in their average observability. Also, i faces a trade-off between the potential income, and the added variation of income between periods. If the conquest of one of the remaining plots would allow i to be attacked by another state (not in the picture), the visualized 'after war'-state is a new equilibrium.

Figure 3: *Stylized example of two states competing for territory. The plot on the left shows the income/budget of the states over time. The right visualization displays the observability of soil quality in two states, before and after i's attack on the southeastern plot.*

$$\frac{\partial \, \mathrm{E}(\Delta_m)}{\partial q_m} > 0 \tag{22}$$

The probabilities of the land signal (6) induces that the higher the land observability, the higher is the possibility that any state j_1 cannot defend all of its plots. Therefore, Δ_m is negatively dependent on the average soil observability of its owner.

Proposition 2. *States with initially random area and a high average soil observability η are larger in equilibrium*

Proof. See appendix. A stylized example is provided in Figure 3. The general intuition is the following. Conquering territory comes with an increase in expected income. However, if the observability of conquered territory decreases the average observability of the victorious state, the variance of income between periods increases. This higher uncertainty in budget induces a higher risk that other states can afford to pay the costs of attack. Therefore, a lower observability leads to a higher vulnerability of a states area, and state rulers have to trade this off against the added expected income. □

This leads us to the final proposition, namely the defensibility of city states,

Proposition 3. *The defense of a city state depends on the relationship of agricultural vs. crafts technology, as well as the soil suitability and observability of its neighbors.*

Proof. See appendix. □

III. Empirical Analysis

The empirical analysis is based on the digitized map of the territories of the HRE in 1378 originally printed in "Carl Wolff's historischer Atlas" (Wolff, 1877) and shown in Figure 1. To the best of our knowledge, this map is the most detailed political map of the medieval HRE available. In particular, it is much more detailed than the maps used by previous studies on the origins and evolution of states in Europe like e.g., Abramson (2016). This gives us a very complete picture of the actual political fragmentation in the medieval HRE than was previously possible.

We employ exogenous spatial grids to rule out endogeneity of state size. The empirical analysis is conducted on grid cell level, with 385 grid cells of 2,500 km ^{2} being the observational units upon which all variables are aggregated. The number of states and the length of borders (in km) in each grid act as the dependent variables. When testing the impact of agricultural observability on the formation of city states, a dummy for grid cells with city states and a variable reporting the actual number of city states within a grid are employed as dependent variables.

I. Dependent Variables

Our dependent variables are the number of territories and the length of all territory borders in a 50km$*$50km (2,500 km^2) grid.[23] Both are calculated using GIS software and are based on the digitized map of the Holy Roman Empire printed in Wolff (1877).[24] The borders and the name of the territories in the map are cross-checked with maps in other atlases like Darby and Fullard (1978), and Stier et al. (1956), as well as with the "Historisches Lexikon der deutschen Länder" (Historical Encyclopedia of German States) (Köbler, 1988) which provides information about the history of every sovereign state that has ever existed in the German Lands (i.e., in the HRE, the German Empire and the Federal Republic of Germany).

Figure 4 overlays onto the HRE the 385, 2,500 km^2 grid cells that will be our observational units in the subsequent empirical analysis. It also shows city states in red and ecclesiastical territories in gray. The number of territories and border-length per grid are calculated using the QGIS zonal statistics tool.

As is evident from the figures, both variables are highly correlated with each other (the bivariate correlation coefficient is 0.93). According to the number of territories and border-length per 2,500 km^2 political fragmentation is highest in the south west of the Holy Roman Empire, in today's southern and middle Germany and in Switzerland. This corresponds to the fact that most of the city states are located in the same area. Moreover, it is low in the east and the north of the Holy Roman Empire where large states like Austria (Habsburg), Bohemia or Brandenburg are located.

Figure 5a shows the number of territories and Figure 5b the border-length per grid.

[23] The grid is created using a projected coordinate system (WGS 1984 UTM Zone 32N). This ensures that all grids are equally large. To ensure that our results are not driven by this arbitrary grid cell size in Appendix C.1, Table C.1 we present estimates using larger grid cells of 1,000 km^2. It turns out that the results even tend to become strong when those large grid cells are used as observational units.

[24] Note that the map excludes the northern Italian parts of the HRE that are thus also not considered in this analysis.

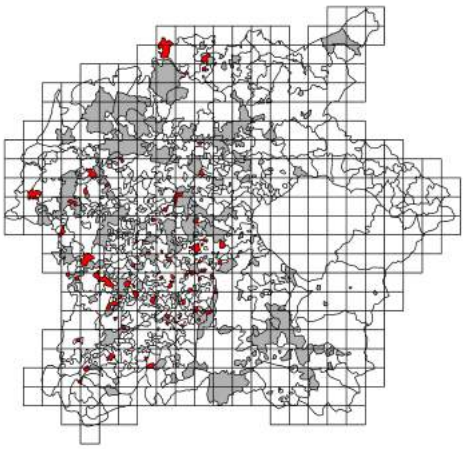

Note: This figure shows the sovereign territories of the HRE in 1378. City states are indicated in red and ecclesiastical territories in gray. The territories of the HRE are overlaid by a net of grid cells of 2,500 km^2 size.

Figure 4: *The Holy Roman Empire in 1378 and the 2,500 km^2 Grid Cells*

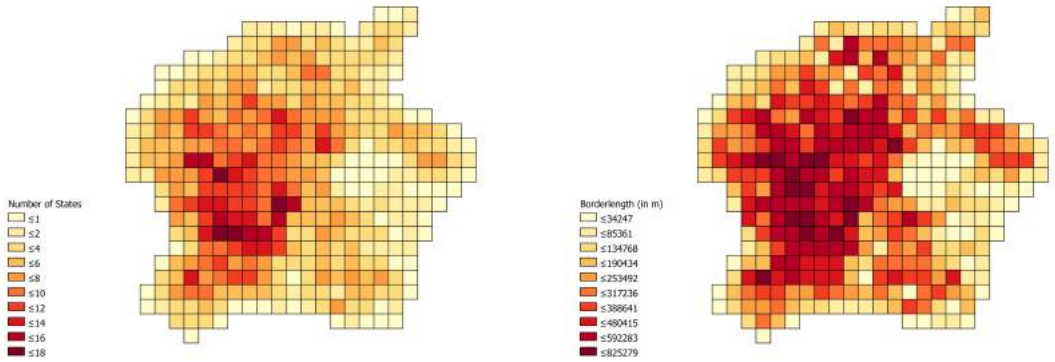

(a) *Number of Territories* **(b)** *Border-Length*

Note: This figure shows the distribution of the number of territories (Panel (a)) and border-length (in km) (Panel (b)) among the 385 grid cells used for the empirical analysis.

Figure 5: *Number of Territories and Border-Length per Grid*

II. Caloric Observability Index

To measure observability, we propose an index that measures divergence from perfect observability, which captures the deviation from the perfect state planner's signal as proposed in equation 6 of the theoretical framework. This measure of observability of agricultural output is based on the caloric suitability index developed in Galor and Özak (2014) and Galor and Özak (2015).[25] This

[25]The caloric suitability index can be downloaded here: `http://ozak.github.io/Caloric-Suitability-Index/`, accessed on April, 24th 2016.

index provides the maximum caloric yield per hectare per year for each grid cell on a resolution of 300 arc seconds (0.083 degrees or around 85 km^2). It assumes that in any data point, the crop with the maximum caloric yield is cultivated.[26] The maximum is derived out of the 49 different crops for which the Global Agro-Ecological Zones (GAEZ) project of the Food and Agriculture Organization (FAO) provides global crop yield estimates. Those estimated crop yields (given in tons, per hectare, per year) are converted into calories using information on the caloric content of the respective crops available from the United States Department of Agriculture Nutrient Database for Standard Reference. The commonly used agricultural suitability measures of Ramankutty et al. (2002). or Zabel et al. (2014), measure the fraction of each grid cell that is suitable for agriculture in terms of probability. Compared to those standard measures, the caloric suitability index has several advantages. First, equally suitable land can have very different caloric yields, as land that is suitable for agriculture will not necessarily be suitable for the crops with the highest caloric yields. In a Malthusian subsistence society, the main purpose of agricultural activities was to feed the population, so the caloric yield is central. Second, the caloric suitability index accounts for the fact that prior to the discovery of the New World not all of the 48 crops incorporated in the GAEZ database were actually available (e.g. potatoes were not available in Europe). Finally, the index is not endogenous to human activities, since Galor and Özak (2014) calculate the potential caloric yields assuming low level of inputs and rain-fed agriculture (it abstracts from irrigation methods) and agro-climatic constraints exogenous to human activities.[27]

We introduce our measure of *Caloric Observability* **(COI)**, defined for a cell in row r and column c of a raster based on the maximum caloric suitability index[28] as

(r-1,c-1)	(r-1,c)	(r-1,c+1)
(r,c-1)	(r,c)	(r,c+1)
(r+1,c-1)	(r+1,c)	(r+1,c+1)

$$Caloric\,Observability(r,c) = \sqrt{\sum_{i=(r-1)}^{(r+1)} \sum_{j=(c-1)}^{(c+1)} \left[CSI_{(i,j)} - CSI_{(r,c)}\right]^2}, \tag{23}$$

For each column c and each row r, we derive the variance between the caloric suitability CSI and that of its neighboring fields. If this variance is zero, measuring caloric suitability of one field would perfectly predict the suitability of its neighboring fields, and caloric observability is zero. With an increase in between-neighbor differences, the relationship between factor input and output becomes less observable, and the peasants' effort therefore harder to observe. Hence, high values of the COI correspond to low observability and vice versa.

Another advantage of the most recent agricultural suitability measure as provided by Zabel et al. (2014) is its higher spatial resolution of 30 arc seconds (equivalent to a grid cell of around 0.86 km^2 size on the equator).

[26] We use the version of the index that does not include crops with zero productivity in the respective grid cell for the calculation of the average caloric yields. As a robustness check we run regressions using the average caloric yield per grid cell taking into account the caloric yields of all crops that can be cultivated in the respective grid cell. Results are reported in Table C.2 in the Appendix.

[27] The spatial distribution of maximum caloric suitability among the territories of the late medieval HRE is depicted in Figure B.2 in the Appendix.

[28] The reader may recognize this specification, as it is strongly related to the concept of terrain ruggedness as proposed by Riley et al. (1999). This allows the usage of tools already implemented in QGIS or other GIS software.

The spatial distribution of the caloric observability on territory and grid level is depicted in Figures 6a and 6b. It fits with the distribution of political fragmentation as depicted in Figure 5. Observability of agricultural output is higher in the south than in the north, while it seems that the medium level of caloric suitability in the eastern regions corresponds to large states and not to medium sized ones—although this is almost only driven by Bohemia and Moravia.

A descriptive overview of the data set used for the empirical analysis including the dependent variables, the Caloric Observability Index and all the control variables can be found in the Appendix Table A.1.

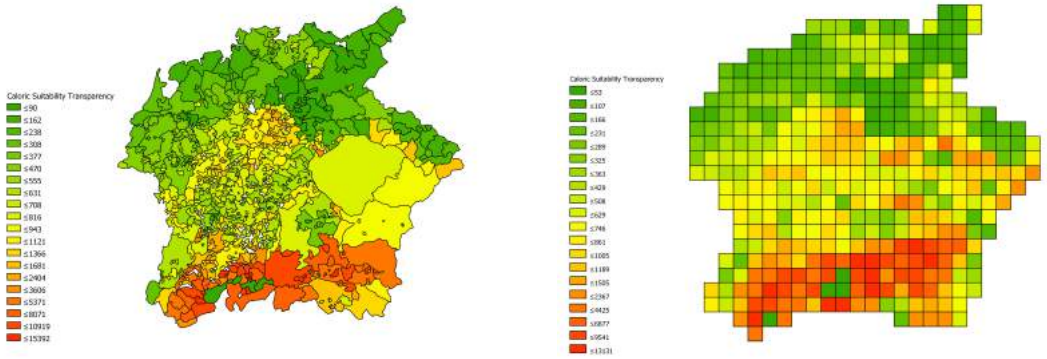

(a) *Maximum Caloric Observability per Territory* **(b)** *Maximum Caloric Observability per Grid*

Note: Panel (a) shows the distribution of caloric (agricultural output) observability among the territories in the HRE and among the grid cells (Panel (b)). The higher caloric observability (the smaller the values of the variable are) is, the more dark-green colored the territories are. The lower caloric observability is (the higher the values of the variable are), the darker-red the territories are colored.

Figure 6: *Caloric Observability*

III. Empirical Strategy

We test proposition 2 running cross-sectional regressions with the number of territories, and the border-length (in km) per grid as dependent variables and the caloric observability index as independent variable. As observability of agricultural output is orthogonal to economic activities, political institutions and human activity in general, the endogeneity problem is not such a crucial issue as in many other empirical studies. Nonetheless, there still could be a third (and unobserved) factor positively correlated with both caloric observability and political fragmentation. This would bias our empirical estimates. To address this, we include several control variables in the regression specification. Additionally, we define a net of larger grid cells of 250,000 km^2 size and add dummy variables indicating to which 250,000 km^2 grid each smaller 2,500 km^2 grid belongs. Hence the larger grid dummies act as some kind of regional fixed effects and thus enable us to further reduce heterogeneity between the different smaller grids. We estimate

$$Political\ Fragmentation_{ic} = \alpha + \beta ln(COI_{ic}) + \gamma' \mathbf{X_{ic}} + \delta_c + \epsilon_{ic} \tag{24}$$

using OLS and Poisson regressions (in the case of the number of territories as dependent variable).

$Political\ Fragmentation_{ic}$ is one of the two measures of political fragmentation, i.e., either the number of territories or the border length in 2,500 km^2 grid cell i and 250,000 km^2 grid cell c. $ln(COI_{ic})$ is the natural logarithm of the caloric observability index and X_{ic} is a vector of control variables comprising the minimal latitudinal and longitudinal coordinates of each small grid i, its average elevation, terrain ruggedness, the length of Roman roads and rivers within the grid cell (in km), a variable indicating the share of ecclesiastical states in a grid, a variable documenting the number of battles that had taken place within the area of a grid cell in the years 800–1378 as well as the average caloric suitability index of Galor and Özak (2014) itself.[29] These controls were proposed as determinants of political fragmentation, city location and state capacity by other studies such as Abramson (2016); Bosker et al. (2013); Dincecco and Gaetano Onorato (2016); Hoffman (2015); Kitamura and Lagerlöf (2015); Karaman and Pamuk (2011). To capture the general trend of larger territories in the north and east of the HRE, we control for longitude and latitude.[30] δ_c are 250,000 km^2 grid cell fixed effects accounting for regional unobserved heterogeneity and ϵ_{ic} is the error term.

We continue with testing proposition 1, that low observability of agricultural output gives rise to the emergence of city states. First, a dummy variable "City State" equal to one if a grid cell includes at least one city state within its area and second a variable "Number of City States" reporting the exact number of cities states within each grid cell. These variables were estimated as

$$City_{ic} = \alpha + \beta ln(COI_{ic}) + \gamma' \mathbf{X_{ic}} + \delta_c + \epsilon_{ic}, \tag{25}$$

$City_{ic}$ being either "City State" dummy or the "Number of City States" variable. The other variables are identical to equation 24. If the "City State" dummy is the dependent variable, we estimate equation 25 as linear probability model or probit model—in the latter case we report the results as average marginal effects. If the number of city states is the dependent variable, we use OLS and Poisson regression as this variable is a count variable.

IV. Results

Table 1 shows the results of estimating equation 24 with the number of territories within each grid cell as dependent variable. Column (1) reports the bivariate regression without any further control variables or fixed effects. From column (2) onward, 250,000 km^2 grid cell fixed effects are included in each regression and additionally from each column to the next more and more control variables are added in groups. Caloric observability is always significant and has a positive coefficient meaning that (according to the estimate in column (6)) a one percent increase in caloric observability (a one percent decrease in the caloric observability Index) decreases the number of states by 0.47 and a one standard deviation (1.397) increase in observability decreases the number of territories by around 0.66 which is sizeable given that the average number of territories in a grid is 5.4. The added covariates do actually increase the size of the coefficient and, hence, the

[29] The sources and exact definitions of all those variables as well as their descriptives are provided in the Data Appendix.
[30] A descriptive overview of all these variables is provided in Appendix B, Table B.1.

effect of caloric observability on political fragmentation is robust to controlling for observables. Looking at the covariates themselves, only elevation, terrain ruggedness and the ecclesiastical states dummy are robustly significant underlining the particularities of ecclesiastical territories (a special type of state only existing in the HRE) and the importance of geography for political fragmentation.

Table 1: *Observability of Agricultural Output and the Number of Territories*

Dep. Var.	Number of Territories					
	(1)	(2)	(3)	(4)	(5)	(6)
ln(Caloric Observability)	0.330***	0.306***	0.391***	0.339***	0.5174***	0.4737***
	(0.103)	(0.118)	(0.115)	(0.117)	(0.0966)	(0.107)
Longitude			-0.002	-0.0019	0.0006	0.0005
			(0.000)	(0.000)	(0.000)	(0.000)
Latitude			-0.0000	0.0015	0.0012	0.0016
			(0.000)	(0.000)	(0.000)	(0.000)
Elevation				0.00542***	0.00403***	0.00476***
				(0.001)	(0.001)	(0.001)
Terrain Ruggedness				-0.0127***	-0.0129***	-0.0130***
				(0.003)	(0.003)	(0.003)
Roman Roads (km)					0.00536	0.00521
					(0.004)	(0.004)
Rivers (km)					-0.00401	-0.00387
					(0.003)	(0.003)
Share of Ecclesiastical States					1.659***	1.656***
					(0.119)	(0.120)
Battles					0.462	0.463
					(0.535)	(0.539)
ln(Caloric Suitability (Pre-1500))						0.583
						(0.710)
500 km Grid Fixed Effects	No	Yes	Yes	Yes	Yes	Yes
Observations	385	385	385	385	385	385
R^2	0.014	0.302	0.306	0.337	0.614	0.615

Notes. Robust Standard errors are reported in parentheses. Coefficient is statistically different from zero at the ***1 %, **5 % and *10 % level. The unit of observation is a grid cell of 2,500 km^2 size. All regressions include a constant not reported as well as seven 250,000 km^2 grid cell fixed effects each of them being equal to one if one of the 2,500 km^2 is located within the respective 250,000 km^2 grid cell.

Table 2 reports the results for border-length as alternative dependent variable. In general, results are similar to those in Table 1 and caloric observability remains statistically and economically significant in every regression. Here, the results imply that a one percent decrease in caloric observability increases the length of borders within a grid by about 20km, which seems to be a relevant effect given that the average border is around 260 km long.

Table 2: *Observability of Agricultural Output and Border-Length*

Dep. Var.	Border-Length (km)					
	(1)	(2)	(3)	(4)	(5)	(6)
ln(Caloric Observability)	15.16***	16.60***	19.67***	24.55***	20.18***	19.65***
	(5.215)	(6.244)	(6.308)	(6.411)	(5.305)	(5.635)
Longitude			-0.135*	-0.132*	-0.0227	-0.0240
			(0.072)	(0.069)	(0.0527)	(0.052)
Latitude			0.0982	0.167**	0.143**	0.147**
			(0.0748)	(0.0728)	(0.063)	(0.069)
Elevation				0.222***	0.158***	0.165**
				(0.063)	(0.049)	(0.069)
Terrain Ruggedness				-0.479***	-0.473***	-0.474***
				(0.161)	(0.131)	(0.132)
Roman Roads (km)					0.175	0.174
					(0.168)	(0.168)
Rivers (km)					-0.228	-0.227
					(0.162)	(0.163)
Share of Ecclesiastical States					74.57***	74.54***
					(6.092)	(6.098)
Battles					37.17	37.18
					(22.66)	(22.70)
ln(Caloric Suitability (Pre-1500))						5.878
						(31.06)
500 km Grid Fixed Effects	No	Yes	Yes	Yes	Yes	Yes
Observations	385	385	385	385	385	385
R^2	0.013	0.250	0.263	0.287	0.537	0.537

Notes. Robust Standard errors are reported in parentheses. Coefficient is statistically different from zero at the ***1 %, **5 % and *10 % level. The unit of observation is a grid cell of 2,500 km^2 size. All regressions include a constant not reported as well as seven 250,000 km^2 grid cell fixed effects each of them being equal to one if one of the 2,500 km^2 is located within the respective 250,000 km^2 grid cell.

We conduct a battery of robustness checks to ensure that our results are robust to different estimation techniques, observability measures and smaller grid area (40,000 km^2 instead of 250,000 km^2). Results of the robustness checks are available in Table 3. There, in columns (1) and (2) we test whether the results of Table 1 column (6) hold if we do not include 250,000 km^2 grid fixed effects 40,000 km^2 grid fixed effects exploiting only variation in political fragmentation within a smaller, more homogeneous geographic area. The results hold. In fact, the estimated coefficients are even larger. Unobserved heterogeneity seems to have—if anything—downward biased our estimates.

Table 3: *Observability of Agricultural Output and Political Fragmentation—Robustness*

Dep. Var.	Number of Territories		Border-Length (km)		Number of Territories			Border-Length (km)	Number of Territories
	(1)	(2)	(3)	(4)	(5)	(6)	(7)	(8)	(9)
Robustness Check	More grid fixed effects		Clustered Standard Errors		Poisson Regression	Alternative Transparency Measure			Accounting for Climate Change
Method	OLS				Poisson	OLS	Poisson	OLS	
ln(Caloric Transparency)	0.448***	0.448***	0.474***	25.92***	0.104***				0.450***
	(0.149)	(0.149)	(0.170)	(9.214)	(0.03)				(0.127)
ln(Soil Transparency)						0.178	0.135**	25.87**	
						(0.237)	(0.06)	(12.31)	
500km Grid Fixed Effects	No	No	Yes	Yes	Yes	Yes	Yes	Yes	Yes
200km Grid Fixed Effects	Yes	Yes	No	No	No	No	No	No	No
Full Controls	Yes	Yes	Yes	Yes	Yes	Yes	Yes	Yes	Yes
Observations	385	385	385	385	385	385	385	385	385
R^2 Pseudo R^2	0.633	0.633	0.410	0.363	0.19	0.439	0.212	0.411	0.408

Notes. Robust Standard errors are reported in parentheses. Coefficient is statistically different from zero at the ***1 %, **5 % and *10 % level. In columns (3) and (4) standard errors clustered on 40,000 km^2 grid cell level are reported. The unit of observation is a grid cell of2,500 km^2 size. All regressions include a constant not reported. In columns (1) and (2) thirty-three 40,000 km^2 grid cell fixed effects each of them being equal to one if one of the 2,500 km^2 grids is located within the 40,000 km^2 grid cell are included. In columns (3)–(9) seven 2,500 km^2 grid cell fixed effects each of them being equal to one if one of the 2,500 km^2 is located within the 250,000 km^2 grid cell are included. The set of full controls encompasses minimum and longitude and latitude of a grid cell, its average elevation and terrain ruggedness, the length of Roman roads and rivers within the grid cell (in km) a variable reporting the share of ecclesiastical states within a grid cell, and the number of battles that have taken place within a grid cell between 800 AD and 1378 AD. Finally we control for the average caloric suitability of a grid cell's soil. In columns (5) and (8) Pseudo R^2 instead of R^2 is reported. In column (9) each observation is inversely weighted by its difference between the average temperature in 800–1378 and 1961–1990.

In columns (3) and (4) we re-estimate column (6) of Tables 1 and 4 with standard errors clustered on 40,000 km^2 grid level to account for the fact that observations, within these areas, are not independent from each other. The results remain highly significant when clustered standard errors are used. In column (5) we account for the fact that number of territories is a count variable. We repeat the regression in column (6) of Tables 1 this time applying Poisson regression instead of OLS. The positive coefficient remains highly significant.

In columns (6)–(8) we use an alternative measure for observability of agricultural output, namely LSA observability. The LSA observability measure is calculated in the same way as the caloric observability index but it is not based on the caloric suitability index of Galor and Özak (2014) but on the (*average*) soil suitability measure of Zabel et al. (2014).[31] As discussed above, compared to the caloric suitability index, agricultural suitability measures have various shortcomings, especially in an historical analysis like the present one. However, the agricultural suitability data of Zabel et al. (2014) is available at a much lower spatial resolution and hence yields more variation in LSA observability when compared to the caloric suitability index. Additionally, and due to the fact that agricultural suitability is a standard variable in the empirical analysis of economic development, it is valuable to use this alternative index as a robustness check. Results suggest that there is also a significantly positive relationship between the number of territories but not on border-length in a grid cell. However, when estimated with OLS, we also do not find a significant effect of LSA observability on the number of territories (column (6)). Even if significant the effect seems to be smaller than with caloric observability. Nevertheless, as LSA observability is noisier and moreover endogenous to human activities, we emphasize the results obtained with caloric observability.

In column (9) we address the fact that despite various adjustments to account for historical conditions, the CSI does not take into account historical climatic conditions. In general we think, that this is not a severe problem as Galor and Özak (2015) show that most of the variation in the CSI does actually come from the soil quality part and not from the climatic part. Even more, our observability does capture variation in caloric yields not caloric yields themselves. If climatic conditions differed between the late medieval period and today, these differences could only make our measure invalid if they would lead us to systematically overstate the observability of caloric output in some areas of the grid and not in others. Given that climatic changes do not usually affect small areas like our grid cells differently, this seems unlikely. However, to ensure that our results are not biased by regionally different intensities of climate change between the 14th century and today we consult the historical climate data set of Guiot and Corona (2010). They constructed a grid cell database of historical European temperatures and their deviations from the average temperature in 1960–1990. We use this data set to calculate, for each grid cell, the average temperature deviation in the period from 800 to 1378.[32] We re-run the regression in Table 1, column (6), this time inversely weighting each grid cell by its temperature deviation from the 20th century. This ensures that grid cells in which the medieval temperature deviates stronger from today—and hence, the caloric yields might be measured with less precision—get lower weights. Thus, this procedure minimizes the bias that could arise from differences between the medieval climate and today's climate. We find that the coefficient only slightly declines and

[31] The exact definition of the soil suitability data as well as its descriptives are available in Appendix B.

[32] To calculate the average temperature deviations for each grid we follow the interpolation procedure of Anderson et al. (2016) by filling in missing values with the inverse distance weighted average temperature of the twenty-four nearest neighbor grid points.

remains highly significant. This suggests that the bias introduced by climate change is at best very small.

Now, we come to the results of estimating equation 25 which allows us to assess whether there is a significant positive relationship between the emergence of city states and caloric observability. Results are reported in Table 4. In columns (1)–(4) the "State City" dummy is the dependent variable and thus, we test whether caloric and LSA observability are significant predictors of city state location. When estimating a linear probability model (columns (1) and (2)) it looks like a one percent increase of caloric observability decreases the probability that a grid cell has at least one city state in its area by around 3.5%. Correspondingly, a one standard deviation increase (1.397) decreases the probability of a city state by around 5%. When estimating a probit model, we found even slightly larger effects suggesting an decrease in probability of a city state of around 10% regardless of whether we use caloric or LSA observability measures.[33]

Regarding the number of city states in each grid (columns (5)–(8)) the results are more ambiguous. In the case of OLS regressions (columns (5) and (6)) we find significant positive effects implying that when caloric observability decreases (the COI increases) by one percent the number of city states in a grid increases by around 0.5. When estimating Poisson regressions to account for the count data nature of the dependent variable we do only get a marginally significant coefficient when using LSA observability but not when using the preferred caloric observability (columns (7) and (8)).

The results provide strong empirical support for our theoretical propositions and highlight the importance of observability of agricultural output for political fragmentation and the occurrence of city states in the medieval HRE.

[33]Note, that in the probit regressions two grid cell dummies (for grid cells 6 and 8) were perfect predictors and hence, both dummy variables and the observations within these grid cells are removed. In consequence, the sample size is reduced to 318.

Table 4: *Observability of Agricultural Output and the Formation of City States*

Dep. Var.	City State				Number of City States			
	(1)	(2)	(3)	(4)	(5)	(6)	(7)	(8)
Method	OLS		Probit		OLS		Poisson	
Standard Errors	Robust	Clustered	Robust	Robust	Robust	Clustered	Robust	Robust
ln(Caloric Observability)	0.0344***	0.0344**	0.118***		0.0460**	0.0460**	0.453	
	(0.011)	(0.015)	(0.042)		(0.021)	(0.018)	(0.305)	
ln(LSA Observability)				0.0928*				0.447*
				(0.049)				(0.255)
500 km Grid Fixed Effects	Yes	Yes	Yes	Yes	Yes	Yes	Yes	Yes
Full Controls	Yes	Yes	Yes	Yes	Yes	Yes	Yes	Yes
Observations	385	385	318	318	385	385	385	385
R^2 or Pseudo R^2	0.275	0.275	0.252	0.269	0.278	0.278	0.314	0.339

Notes. Robust Standard errors are reported in parentheses. Coefficient is statistically different from zero at the ***1 %, **5 % and *10 % level. In columns (3) and (4) standard errors clustered on 200 km^2 grid cell level are reported. The unit of observation is a grid cell of 2,500 km^2 size. In columns (3)and (4) average marginal effects and Pseudo R^2 instead of R^2 are reported. All regressions include a constant not reported. In columns (1) and (2) 33 40,000 km^2 grid cell fixed effects each of them being equal to one if one of the 2,500 km^2 is located within the 40,000 km^2 grid cell are included. In columns (3)–(8) seven 250,000 km^2 grid cell fixed effects each of them being equal to one if one of the 2,500 km^2 is located within the 250,000 km^2 grid cell are included. The set of full controls encompasses minimum and longitude and latitude of a grid cell, its average elevation and terrain ruggedness, the length of Roman roads and rivers within the grid cell (in km) and the number of battles that have taken place within a grid cell between 800 AD and 1378 AD. Finally we control for the average caloric suitability of a grid cell's soil.

V. Conclusion

This paper has studied the determinants of political fragmentation in the Holy Roman Empire, the *"irregular Monstrosity"* in the middle of Europe (von Pufendorf, 1667). We were able to theoretically and empirically show that the observability of agricultural output, via its impact on taxation capacity and the political structure of states, was a primary determinant of state size in pre-modern central Europe. Low agricultural observability limited state capacity, fostered political fragmentation, and the emergence and survival of city states. These city states were the settings for many important political and economical innovations (like guilds or printing), proto-industry, and revival trade during the late Middle Ages. Hence, we have contributed to a better understanding of the origins of Europe's unique urban network and later economic take-off.

Our results provide evidence for the interaction of agriculture, climate, and geography in explaining political outcomes like state capacity or regime. This adds a new perspective to the existing large and influential literature that links geography, climate and agriculture to long-run differences in economic outcomes (Diamond, 1999; Olsson and Hibbs, 2005). Moreover, our study provides evidence for the link between soil transparency and political institutions outlined in Mayshar et al. (2014) that inspired our analysis.

Additionally, we have proposed a GIS measurement of observability of agricultural output. As this index is well grounded in theoretical economic reasoning, it is potentially useful for several other research endeavors in economic history, and long-run development.

Finally, the question of the persistence and long-run consequences of political fragmentation remains. Until now, the literature has disagreed on whether political fragmentation is harmful or beneficial for long-run economic development. This disagreement might to some extent be caused by the fact that many of the arguments that have been made were never thoroughly empirically tested. A central aspect of Mayshar et al. (2014), namely that an alternative response to adjusting state size to fit the observability of the soil is the adjustment of the political institutions, through more oppression, or through positive incentives to peasants, remains to be tested.

References

Abramson, S. (2016). The economic origins of the territorial state. *International Organization, forthcoming*.

Acemoglu, D. and Robinson, J. A. (2006). Economic backwardness in political perspective. *American Political Science Review*, 100(1):115–131.

Alesina, A. and Spolaore, E. (1997). On the number and size of nations. *Quarterly Journal of Economics*, 112(4):1027–1056.

Allen, R. (2009). *The British Industrial Revolution in Global Perspective*. New Approaches to Economic and Social History. Cambridge University Press.

Anderson, P. (1978). *Von der Antike zum Feudalismus. Spuren der Übergangsgesellschaften*. Suhrkamp Verlag, Frankfurt am Main.

Anderson, R. W., Johnson, N. D., and Koyama, M. (2016). Jewish persecutions and weather shocks: 1100–1800. *Economic Journal, forthcoming*.

Ang, J. (2015). What drives the historical formation and persistent development of territorial states. *Scandinavian Journal of Economics*, 117(4):1134–1175.

Bentzen, J. S., Kaarsen, N., and Wingender, A. M. (2016). Irrigation and autocracy. *Journal of the European Economic Association, forthcoming*.

Bloch, M. (1982). *Die Feudalgesellschaft*. Propyläen Verlag, Berlin.

Bockstette, V., Chanda, A., and Putterman, L. (2002). States and marktes: The advantage of an early start. *Journal of Economic Growth*, 7(4):347–369.

Bolton, P. and Roland, G. (1997). The breakup of nations: a political economy analysis. *Quarterly Journal of Economics*, pages 1057–1090.

Borcan, O., Olsson, O., and Putterman, L. (2014). State history and economic development. evidence from six millenia. *University of Gothenburg Working Papers in Economics, No. 602*.

Bosker, M. and Buringh, E. (2016). City seeds: Geography and the origins of the european city system. *Journal of Urban Economics, forthcoming*.

Bosker, M., Buringh, E., and Van Zanden, J. L. (2013). From baghdad to london. unraveling urban development in europe, the middle east, and north africa, 800–1800. *Review of Economics and Statistics*, 95(4):1418–1437.

Bradbury, J. (2004). *The Routledge Companion to Medieval Warfare*. Routledge, London.

Cantoni, D. (2012). Adopting a new religion: the case of protestantism in 16th century germany*. *The Economic Journal*, 122(560):502–531.

Clark, C. (2007). *Iron Kingdom: The rise and downfall of Prussia, 1600–1947*. Penguin Books, New York NY.

Darby, H. C. and Fullard, H., editors (1978). *The New Cambrigde Economic History Atlas*. Cambridge University Press, Cambridge, UK.

Diamond, J. (1999). *Guns, Germs and Steel: The Fates of Human Societies*. W.W. Norton, New York NY.

Dincecco, M. (2015). The rise of effective states in europe. *Journal of Economic History*, 75(3):901–918.

Dincecco, M. and Gaetano Onorato, M. (2016). Military conflict and the rise of urban europe. *Journal of Economic Growth, forthcoming*.

Eisenstadt, S. and Rokkan, S. (1973). *Building States and Nations*. Sage Publications, Beverly Hills CA.

Fried, J. (2013). *Das Mittelalter*. C. H. Beck, Munich.

Galor, O. and Özak, Ö. (2014). The agricultural origins of time preference. Technical report, National Bureau of Economic Research.

Galor, O. and Özak, Ö. (2015). Land productivity and economic development: Caloric suitability vs. agricultural suitability. *Brown University Working Paper*.

Gennaioli, N. and Voth, H.-J. (2015). State capacity and military conflict. *Review of Economic Studies*, 82(4):1409–1448.

Guiot, J. and Corona, C. (2010). Growing season temperatures in europe and climate forcings over the past 1400 years. *PLOS One*, 5(4):1–15.

Heather, P. (2014). *Die Wiedergeburt Roms. Päpste, Herrscher und die Welt des Mittelalters*. J. G. Cotta'sche Buchhandlung Nachfolger, Stuttgart.

Henning, F.-W. (1994). *Deutsche Agrargeschichte des Mittelalters: 9. bis 15. Jahrhundert*. Eugen Ulmer Verlag, Stuttgart.

Hermann, K. (1985). *Pflügen, Säen, Ernten. Landarbeit und Landtechnik in der Geschichte*. Rowohl Taschenbuch Verlag, Reinbek.

Hoffman, P. T. (2015). *Why Did Europe Conquer the World?* Princeton University Press, Princeton NJ.

Huning, T. R. and Wolf, N. (2016). How britain unified germany: Endogenous trade costs and the formation of a customs union. *Mimeo*.

Jacob, M. (2010). Long-term persistence: The free and imperial city experience in germany. *Mimeo*.

Jisheng, Y. (2012). *Tombstone: The untold story of Mao's great famine*. Farrar Straus & Giroux.

Johnson, N. D. and Koyama, M. (2015). States and economic growth: Capacity and constraints. *Mimeo*.

Karaman, K. and Pamuk, S. (2011). Different path to the modern state in europe: The interaction between domestic political economy and interstate competition. *LEQS Paper No. 37/2011*.

Keyser, E. and Stoob, H., editors (1939–1974). *Deutsches Städtebuch. Handbuch städtischer Geschichte*, volume 1–11. Verlag W. Kohlhammer, Stuttgart.

Kitamura, S. and Lagerlöf, N.-P. (2015). Natural borders. *Mimeo*.

Ko, C., Koyama, M., and Tuan-Hwee, S. (2014). Unified china and divided europe. *Mimeo*.

Köbler, G. (1988). *Historisches Lexikon der deuschen Länder. Die deutschen Territorien und reichsunmittelbaren Geschlechter vom Mittelalter bis zur Gegenwart*. C.H. Beck, Munich.

Lameli, A., Nitsch, V., Südekum, J., and Wolf, N. (2015). Same same but different: Dialects and trade. *German Economic Review*, 16(3):290–306.

Lehmann, S. H. (2010). The german elections in the 1870s: why germany turned from liberalism to protectionism. *Journal of Economic History*, 70(01):146–178.

Mayshar, J., Moav, O., and Neeman, Z. (2014). Geography, transparency and institutions. *Mimeo*.

McCormick, M., G., H., G., Z., and Lavash, J. (2013). Roman road network (version 2008). *DARMC Scholarly Data Series. Data Contribution Series No. 2013-5*.

Mieck, I. (1992). Preußen von 1807 bis 1850. Reformen, Restauration und Revolution. In Büsch, O., editor, *Handbuch der Preußischen Geschichte*, volume 2, pages 1–292. Walter de Gruyter, Berlin.

Mitterauer, M. (2002). Die vormoderne Stadt: Asien und Europa im Vergleich. In Feldbauer, P., Mitterauer, M., and Schwentker, W., editors, *Städte als Zentren im mittelalterlichen Europa*,

volume 10, chapter Die vormoderne Stadt: Asien und Europa im Vergleich, pages 60–78. Oldenbourg Verlag, Munich.

Mitterauer, M. (2004). *Warum Europa? Mittelalterliche Grundlagen eines Sonderwegs*. C.H. Beck, Munich.

Mokyr, J. (2011). *The Enlightened Economy: Britain and the Industrial Revolution, 1700-1850* Penguin Books Limited.

Montesquieu, C. (1749). *The Spirit of the Laws*. Chatelain.

North, D. and Thomas, R. (1973). *The Rise of the Western World: A New Economic History*. Cambridge University Press, Cambridge, UK.

Nunn, N. and Puga, D. (2012). Ruggedness: The blessing of bad geography in Africa. *Review of Economics and Statistics*, 94(1):20–36.

Olsson, O. and Hibbs, D. (2005). Biogeography and long-run economic development. *European Economic Review*, 49(4):909–938.

Ramankutty, N., Foley, J., Norman, J., and McSweeney, K. (2002). The global distribution of cultivable lands: Current patterns and sensitivity to possible climate change. *Global Ecology and Biogeography. A Journal of Macroecology*, 11(3):377–392.

Riley, S. J., DeGloria, S. D., and Elliot, R. (1999). A terrain ruggedness index that quantifies topographic heterogeneity. *Intermountain Journal of Sciences*, 5:23–27.

Samuelson, P. A. (1954). The transfer problem and transport costs, ii: Analysis of effects of trade impediments. *Economic Journal*, 64(254):264–289.

Simms, B. (2013). *Europe: The Struggle for Supremacy, from 1453 to the Present*. Penguin Books, London.

Spolaore, E. (2014). The economics of political borders. *Mimeo*.

Stasavage, D. (2011). *States of Credit. Size, Power and the Development of European Politics*. Princeton University Press, Princeton NJ.

Stasavage, D. (2014). Was weber right? the role of urban autonomy in europe's rise. *American Political Science Review*, 108(2):337–354.

Stier, H.-E., Kirsten, E., Wühr, W., Quirin, H., Trillmich, W., Czybulka, G., Pinnow, H., and Ebeling, H., editors (1956). *Westermanns Atlas zur Weltgeschichte* , volume Vorzeit/ Altertum, Mittelalter, Neuzeit. Georg Westermann Verlag, Brunswick.

Talbert, R., editor (2000). *Barrington Atlas of the Greek and Roman World*. Princeton University Press, Princeton NJ.

Temin, P. (2002). The golden age of european growth reconsidered. *European Review of Economic History*, 6(01):3–22.

Tilly, C., editor (1975). *The Formation of National States in Western Europe*. Princeton University Press, Princeton NJ.

von Pufendorf, S. (1667). *Bericht vom Zustande des Teutschen Reichs*. n/a.

von Thünen, J. (1826). *Der isolierte Staat in Beziehung auf Landwirtschaft und Nationalökonomie, oder, Untersuchungen über den Einfluss, den die Getreidepreise, der Reichthum des bodens und die Abgaben auf den Ackerbau ausüben*. Klassiker der Nationalökonomie. Verlag Wirtschaft und Finanzen, Düsseldorf.

Wahl, F. (2015). Participative political institutions and city development 800–1800. *EHES Working Papers in Economic History, No. 73*.

Weber, E. (1976). *Peasants Into Frenchmen: The Modernization of Rural France, 1870-1914*. Stanford University Press.

Wehler, H.-U. (1995). Von der "Deutschen Doppelrevolution" bis zum Beginn des Ersten Weltkrieges 1849-1914(Deutsche Gesellschaftsgeschichte, Bd. 3). *C.H. Beck, Munich*.

Wilson, P. (2016). *The Holy Roman Empire: A Thousand Years of Europe's History*. Allen Lane.

Wilson, P. H. (2009). *The Thirty Years War: Europe's Tragedy*. Harvard University Press.

Wolf, N. (2009). Was Germany ever united? Evidence from intra-and international trade, 1885–1933. *Journal of Economic History*, 69(03):846–881.

Wolff, C. (1877). *Carl Wolff's historischer Atlas*. Reimer Verlag, Berlin.

Zabel, F., Putzenlechner, B., and Mauser, W. (2014). Global agricultural land resources. a high resolution suitability evaluation and its perspectives until 2100 under climate change conditions. *PLOS One*, 9(9):1–12.

Appendix

A. Mathematical Appendix

Theorem. *The quality of the soil, and soil observability, determine state capacity of an agricultural territorial state*

Proof. Assume a sufficient number of peasants in a country, so that we can use the properties of the normal distributed S^*. Also assume that the time horizon t^* is sufficiently large, so that weather shocks even out. Subsistence of peasants negatively depends onη due to punishment to the ruler in case peasant starve, $s(\eta)$ 10. This means that the average output of any field and time period equals the expected value of an average period times the period, so that

$$\begin{aligned}
\frac{t\sum_{m\in N_i}\mathrm{E}(T_{mt})}{mt} &= \frac{\sum_{m\in N_i}\mathrm{E}[A1^{\alpha}S_{mt}^{*(1-\alpha)}-s(\eta)]}{m}\\
&= \frac{\sum_{m\in N_i}A1^{\alpha}\mathrm{E}[S_{mt}^{*}]^{(1-\alpha)}-s(\eta)}{m}\\
&= \frac{1}{m}\sum_{m\in N_i}A1^{\alpha}[\int_{-\infty}^{\infty}S_{mt}^{*}\frac{1}{\eta\sqrt{2\pi}}\mathrm{e}^{-}(\frac{S_{mt}^{*}-S_{mt}}{2\eta})^2\mathrm{d}S_{mt}^{*}]^{(1-\alpha)}-s(\eta)\\
&= \frac{1}{m}\sum_{m\in N_i}\frac{A1^{\alpha}}{\eta\sqrt{2\pi}}[\int_{-\infty}^{\infty}S_{mt}^{*}\mathrm{e}^{-}(\frac{S_{mt}^{*}-S_{mt}}{2\eta})^2\mathrm{d}S_{mt}^{*}]^{(1-\alpha)}-s(\eta)\\
&= \frac{1}{m}\sum_{m\in N_i}\frac{A1^{\alpha}}{\eta\sqrt{2\pi}}[\sqrt{\pi}S_{mt}\eta\mathrm{erf}(\frac{S_{mt}^{*}-S_{mt}}{2\eta})-2\eta^2\mathrm{e}^{-}(\frac{S_{mt}^{*}-S_{mt}}{2\eta})^2]-s(\eta)
\end{aligned}$$

with

$$\mathrm{erf}(x)=\int\frac{2\mathrm{e}^{-x^2}}{\sqrt{\pi}}\mathrm{d}x$$

Comparative statics of land suitability q_m and quality of the signal η yields that

$$\frac{\partial\left[\lim_{\substack{N_i\to\infty\\ t\to\infty}}\left(\frac{T_i^{\Lambda}}{mt}\right)\right]}{\partial\left[\frac{\sum_{m\in N_i}q_m}{m}\right]}>0 \qquad \text{and} \qquad \frac{\partial\left[\lim_{\substack{N_i\to\infty\\ t\to\infty}}\left(\partial\frac{T_i^{\Lambda}}{mt}\right)\right]}{\partial\left[\frac{\sum_{m\in N_i}\eta_m}{m}\right]}<0 \tag{26}$$

so that we established both a positive link between long-run tax revenue and average soil quality, and its observability. □

Proposition 1. *City states bear a lower soil quality, or soil observability, or a combination of the two.*

Proof. State planners are indifferent to the amount of peasants and city residents iff the marginal increase in the certain income from a citizen equals the loss from a peasant that is migrated to a city. State planners trade-off the expected value of agricultural output against the certain tax income from city residents. This means that there exists a marginal soil quality, and also a marginal observability, at which state planners are indifferent,

$$\frac{\partial T_{it}}{\partial N_{it}} = \mathrm{E}\left(Y_{mt}\left(A, q_m, \eta_m, s(\eta_m)\right)\right) - Y_{ct}\left(B\right) - (\tau - 1)(s_0) \tag{27}$$

If state size is constant, and technology is static, the only decision variable states have is to move their subjects from the agricultural sector to the city, and vice versa. Therefore, the only decision variable in the maximization is N_{it},

$$T_i = \max_{N_{it}} \left[\sum_{t=0}^{\infty} \left(\frac{\sum_{m \in N_{it}}^{\infty} \mathrm{E}\left(T_{mt}\right)}{\left(1+\delta\right)^t} \right) + \frac{(z - N_{it}) Y_{ct} - (\tau - 1)\, s_0}{\delta} \right] \tag{28}$$

□

Proposition 2. *States with initially random area bearing a high average soil observability η are larger in equilibrium*

Proof. In addition to the argument for the land quality, an increase in the noise of the taxation increases the variation of tax-income between periods. For the case of $\eta = 0$, output is perfectly observable and taxation is constant for all periods. With any decrease in observability, tax revenue becomes more unpredictable (equations 6 and 7). This increases the probability of losing territory (equation 19). □

Proposition 3. *The defense of a city state depends on the relationship of agricultural vs. crafts technology, and the soil suitability and observability of its neigbors.*

Proof. Tax revenues in cities is independent of soil (equation 14), unlike territorial states (equation 3). The probability of winning a war is dependent on state revenue (equation 19), and the probability of not being able to defend an attack in any period is negatively related to the attacked country's average soil observability. □

B. Data Appendix

B.1. Dependent Variables

The number of territories and the border-length (in km) in each grid are calculated based on a shapefile created from the map "Deutschland beim Tode Karl des IV. im Jahre 1378" ("Germany at the death of Charles IV. in the year 1378") printed in Wolff (1877). The map is shown below in Figure B.1. It does not show the parts of the HRE that are located in northern Italy and it does wrongly include the state of the Teutonic Order to the HRE, which was never actually part of it,

hence when digitizing the map we excluded these area from the resulting shapefile. The map is available here: `http://gei-digital.gei.de/viewer/javax.faces.resource/pdf-icon32.png.xhtml?ln=images/` (accessed on January 22, 2016).

Note: This figure shows the original map of the HRE as printed in Wolff (1877). For our empirical analysis we digitized this map using GIS software.

Figure B.1: *Germany at the Death of Charles IV. in the Year 1378 (Wolff, 1877)*

B.2. The Spatial Distribution of Maximum Caloric Suitability

The spatial distribution of maximum caloric suitability index of Galor and Özak (2014) among the territories of the HRE is depicted in Figures B.2. The caloric suitability index shows low levels of suitability especially in the southernmost part of the HRE (in today's Switzerland Austria and Bavaria), a medium suitability in the north east and middle of the HRE, and the highest suitability in Rhineland and the northeastern parts (that later became the heartland of Prussia).

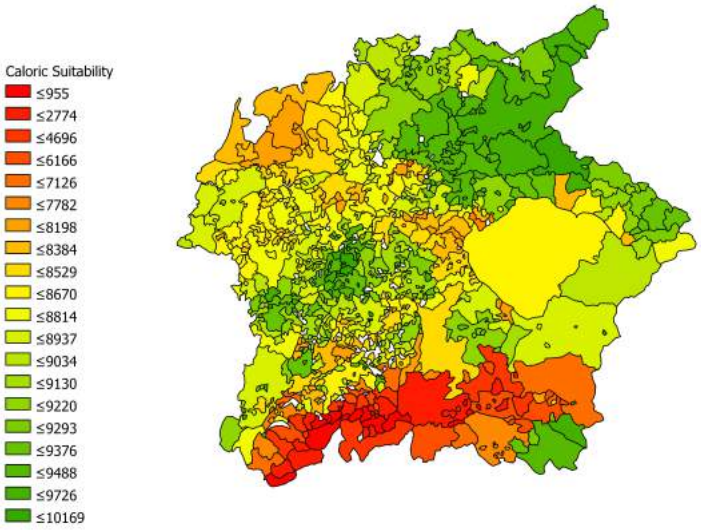

Note: This figure shows the distribution of caloric suitability among the territories in the HRE. The lower the caloric suitability, the darker-red the territories are. The higher the caloric suitability, the darker-green the territories are.

Figure B.2: *Maximum Caloric Suitability in the Territories of the HRE*

B.3. LSA Observability as Alternative Observability Measure

LSA observability is calculated in a similar way to caloric obscurity. It is based on the agricultural suitability measure developed in Zabel et al. (2014). [34] The measure used in the paper is average agricultural suitability in the period 1961–1990. Zabel et al. (2014) measure agricultural suitability by considering climate (temperature, precipitation, solar radiation), soil (pH, texture, salinity, organic carbon content, etc.), and topography (elevation and slope) of a grid cell of 30 arc seconds*30 arc seconds (0.86 km ^{2} at the equator) size. They consider rain-fed conditions as well as irrigation (what could, among other things, give rise to endogeneity issues). To compute agricultural suitability, they contrast these factors with growing requirements of 16 plants (Barley, Cassava, Groundnut, Maize, Millet, Oilpalm, Potato, Rapeseed, Rice, Rye, Sorghum, Soy, Sugarcane, Sunflower, Summer wheat, Winter wheat).

The distribution of average agricultural suitability (cultivation probability) in the territories of the HRE in 1378 AD is shown in Figure B.3. In the southern half of the HRE it is relatively similar to caloric suitability. In the northern part however, there seems to be a negative relationship between agricultural suitability and caloric suitability as caloric suitability seems to be high in the north east of the HRE but agricultural suitability is low there. This suggests that the quality of the soils in the north and north-east of the HRE was not very good for most of the crops considered by Zabel et al. (2014) but that nevertheless the farmers there could cultivate crops allowing a high caloric yield.

[34] The data set is described further here: `http://geoportal-glues.ufz.de/stories/globalsuitability.html` (last accessed on January 22, 2016), where it also can be downloaded.

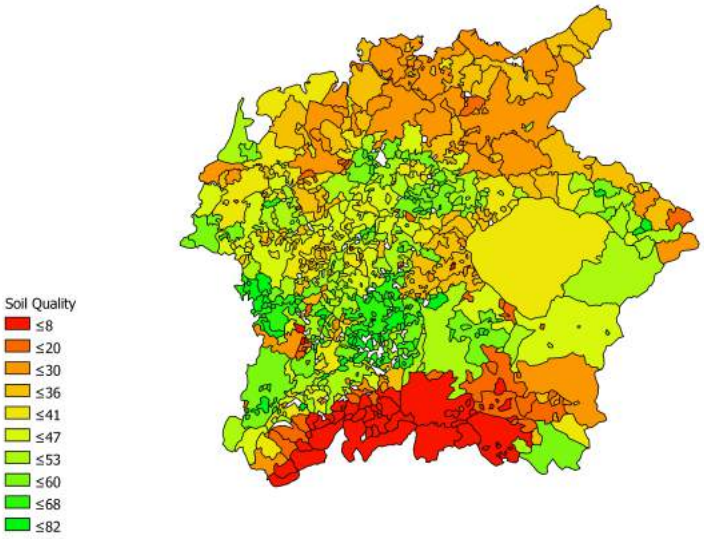

Note: This figure shows the distribution of average agricultural suitability (cultivation probability) among the territories of the HRE. The lower agricultural suitability is, the more dark-red colored the territories are. The higher agricultural suitability is, the darker-green the territories are colored.

Figure B.3: *Agricultural Suitability in the HRE*

Average LSA observability is depicted in Figure B.4a on territory level and in Figure B.4b on grid cell level. The first thing that is evident from the figures is that LSA observability is much less systematically distributed across the HRE, agricultural conditions are the most observable in the south west of today's Germany, in the Rhineland and in the area of today's Saxony. Compared to the LSA observability the differences are highest in the north of the HRE in today's Lower-Saxony and Schleswig-Holstein where we observe high LSA observability but low caloric observability.

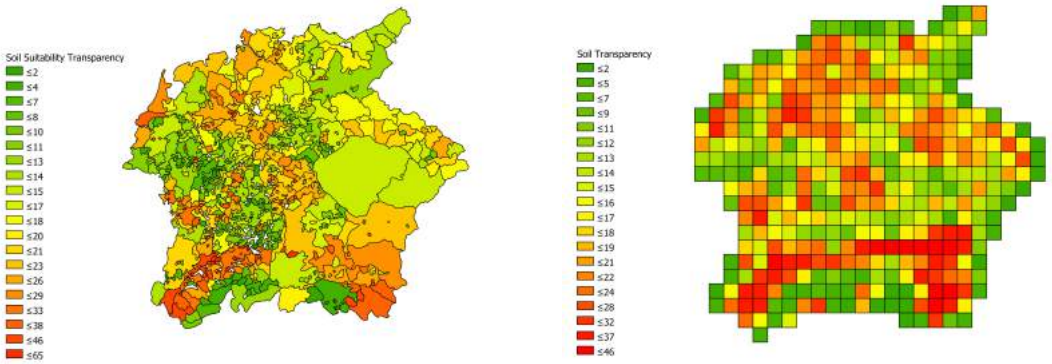

(a) *Territory* **(b)** *Grid Cell Averages*

Note: Panel (a) shows the distribution of average LSA observability among the territories of the HRE and the grid cells (Panel (b)).

Figure B.4: *Soil Observability in the HRE*

B.4. Control Variables

The spatial datasets were each converted into WGS 1984 UTM 32N projection before performing the calculations.

Battles. Number of battles that had taken place within a grid cell between 800 AD and 1378 AD. Information of the date and location of the battles is taken from Bradbury (2004).

City States. Dummy variable equal to one if a grid cell had at least one city state within its area. Information about the location of city states follows the map of Wolff (1877) as well as the information in Köbler (1988), Keyser and Stoob (1974) and Jacob (2010).

Share of Ecclesiastical States. Share of ecclesiastical territories within a grid cell. Information about the location of city states follows the map of Wolff (1877) as well as the information in Köbler (1988).

Elevation. Average elevation of each grid in meters. Data is based on the Digital Elevation Model (DEM) of the U.S. Geological Survey's Center for Earth Resources Observation and Science (EROS), namely the GTOPO30 dataset, which can be downloaded here `https://lta.cr.usgs.gov/GTOPO30` (last accessed May, 30th 2016). The GTOPO30 has a spatial resolution of 30 arc seconds.

Latitude. Minimum longitudinal coordinates of a grid cell in kilometers. Calculated using QGIS.

Longitude. Minimum longitudinal coordinates of a grid cell in kilometers. Calculated using QGIS.

Number of City States. Number of city states within each grid cell, sources are the same as for the "City States" variable (see above).

Rivers (km). Length of rivers in kilometers (small and major) within each grid cell. Provided by the European Environment Agency. We used the union of the datasets for 'large rivers', and the one for 'other large rivers and tributaries', which can each be downloaded here `http://www.eea.europa.eu/data-and-maps/data/wise-large-rivers-and-large-lakes`(last accessed May, 30th 2016).

Roman Roads (km). Length of Roman roads in kilometers within each grid cell. Locations of Roman roads (minor and major) originate from a shapefile included in the "Digital Atlas of Roman and Medieval Civilizations" (McCormick et al., 2013). The shapefile is based on the map of Roman roads in the Barrington Atlas of the Greek and Roman World (Talbert, 2000). It can be downloaded here: `http://darmc.harvard.edu/icb/icb.do?keyword=k40248&pageid=icb.page601659` (last accessed September, 24th 2015).

Terrain Ruggedness. Following Riley et al. (1999) average ruggedness of a grid cells terrain is

calculated as the negative value of the derivative of the ruggedness index of a digital elevation model. The calculations are based on the elevation raster of Nunn and Puga (2012) (see above). Terrain ruggedness was calculated using QGIS.

B.5. Descriptive Statistics

Table B.1: *Descriptive Overview of the Data Set*

Variable	Obs	Mean	Std. Dev.	Min	Max
Agricultural Suitability	385	32.386	19.186	0	72.074
Battles	385	0.039	0.219	0	2
Border-Length (km)	385	260.930	187.006	0	825.279
City State	385	0.190	0.393	0	1
Share of Ecclesiastical States	385	18.061	19.871	0	100
Elevation	385	430.149	480.898	-3.742	2291.378
Latitude	385	5510.429	280.867	4963.026	6063.026
ln(Caloric Observability)	385	6.332	1.397	0	9.483
ln(Caloric Suitability (Pre-1500))	385	7.53	0.583	4	7.954
ln(LSA Observability)	385	2.667	0.732	0	3.858
Longitude	385	631.502	287.485	82.93089	1232.931
Number of City States	385	0.325	0.830	0	5
Number of Territories	385	5.387	3.918	1	18
Rivers (km)	385	40.203	49.676	0	252.564
Roman Roads	385	28.295	58.075	0	246.454
Terrain Ruggedness	385	137.491	190.040	1.91986	767.329

C. Robustness Checks and Additional Results

C.1. Results with Larger Grid Cells

To ensure that the results of the main text are not driven by our arbitrarily chosen grid size of 2,500 km^2 we re-run the regression reported in Table B.1 but this time using larger grid cells with a size of 100km*100km (10,000 km^2) as observational units. The larger grid cells lead to a reduction in the number of observations to 109, which however, should still be enough to get reliable estimates. The number of territories and the caloric observability per grid cell are shown in Figure C.1a and C.1b, respectively.

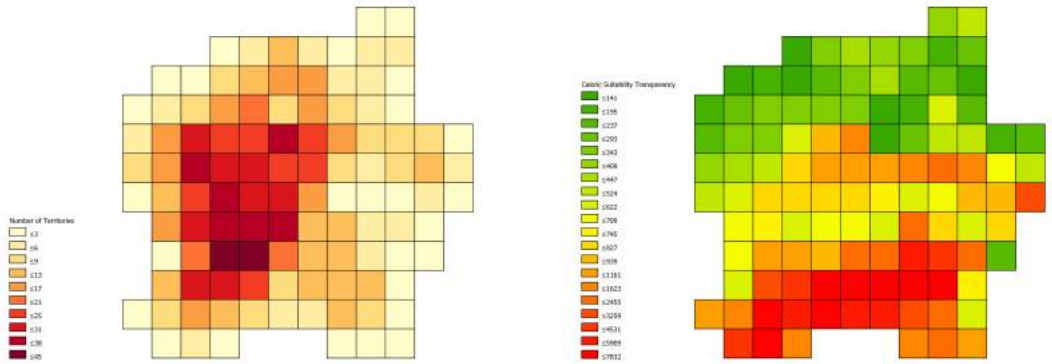

(a) *Number of Territories* **(b)** *Caloric Observability*

Note: Panel (a) shows the distribution of the number of territories among the 385 grid cells used for the empirical analysis. Panel (b) reports the distribution of caloric observability among the grid cells. The lower the caloric observability (the smaller the values of the variable are), the more dark-green the territories are. The higher the caloric observability (the higher the values of the variable are), the darker-red the territories are.

Figure C.1: *Number of Territories and Caloric Observability per 10,000 ^{2} Grid Cell*

In general, both the number of territories and caloric observability show the same pattern as with the smaller grid size. We therefore expect qualitatively similar results, although the precision of the estimation might be lower as sample size and variation in the variables of interest decreases. The results of estimating Table 1 with larger grids are shown in Table C.1. Apart from column (1) caloric observability always shows a significantly positive and actually very large coefficient implying that a one percent increase in the observability index (a decrease in observability) increases the number of territories in a grid by around two. In conclusion, one can say that our results are not driven by the grid cell size.

Table C.1: *Observability of Agricultural Output and the Number of Territories—Larger Grid Cells*

Dep. Var.	Number of Territories					
	(1)	(2)	(3)	(4)	(5)	(6)
ln(Caloric Observability)	1.038	3.199***	2.749**	3.683**	3.014**	2.312**
	(0.665)	(0.946)	(1.097)	(1.845)	(1.491)	(1.482)
Longitude			0.0053	0.0043	0.0026	0.0009
			(0.006)	(0.006)	(0.004)	(0.005)
Latitude			-0.0067	-0.0034	-0.0015	-0.0001
			(0.008)	(0.007)	(0.005)	(0.005)
Elevation				0.0193*	0.0144*	0.0182**
				(0.01)	(0.008)	(0.009)
Terrain Ruggedness				-0.0505*	-0.0424**	-0.0380*
				(0.026)	(0.021)	(0.02)
Roman Roads (km)					-0.0052	-0.0051
					(0.005)	(0.005)
Rivers (km)					0.0000	-0.0004
					(0.004)	(0.004)
Share of Ecclesiastical States					0.1042**	0.095**
					(0.041)	(0.041)
Battles					1.933	1.987
					(1.615)	(1.612)
Caloric Suitability (Pre-1500)						5.570
						(4.126)
500km Grid Fixed Effects	No	Yes	Yes	Yes	Yes	Yes
Observations	109	109	109	109	109	109
R^2	0.012	0.519	0.526	0.552	0.61	0.614

Notes. Robust Standard errors are reported in parentheses. Coefficient is statistically different from zero at the ***1 %, **5 % and *10 % level. The unit of observation is a grid cell of 10,000 km^2 size. All regressions include a constant not reported as well as seven 250,000 km^2 grid cell fixed effects each of them being equal to one if one of the 10,000 km^2 is located within the respective 250,000 km^2 grid cell.

C.2. Results with Average Caloric Observability

In Table C.2 we re-run the regressions of Table 1 this time using average caloric observability as the dependent variable. Hence, we assume that all crops with caloric yield > 0 are actually planted in a grid cell, despite the fact, that it is unlikely that farms will have planted as much of a crop with low caloric yield as of a crop with high caloric yield. We therefore think that the average measure is noisier than the maximum caloric observability used in the main text, although it might also be considered to be a strong assumption that only the crop with the highest caloric yield is actually cultivated in a grid cell. The correlation between both caloric observability measures is around 0.91 and thus very high.

Conversely, results remain qualitatively unaffected by the use of the average caloric observability and imply roughly the same effect as found using maximum caloric observability, i.e. a one percentage increase in average caloric observability decreases the number of territories in a grid

by around 0.5. Hence, our results hold regardless of whether we use average or maximum caloric yields as basis for our caloric observability measure.

Table C.2: *Average Observability of Agricultural Output and the Number of Territories*

Dep. Var.	Number of Territories					
	(1)	(2)	(3)	(4)	(5)	(6)
ln(Average Caloric Observability)	0.211*	0.448**	0.6866***	0.5504**	0.491**	0.491**
	(0.123)	(0.190)	(0.191)	(0.252)	(0.234)	(0.253)
Longitude			-0.0021	-0.0021	0.0005	0.0005
			(0.001)	(0.001)	(0.001)	(0.001)
Latitude			0.00041	0.0016	0.0011	0.0010
			(0.002)	(0.002)	(0.001)	(0.002)
Elevation				0.0046***	0.0034***	0.0033*
				(0.001)	(0.001)	(0.002)
Terrain Ruggedness				-0.0117***	-0.0118***	-0.0118***
				(0.003)	(0.003)	(0.003)
Roman Roads (km)					0.0049	0.0049
					(0.004)	(0.004)
Rivers (km)					-0.0043	-0.0043
					(0.003)	(0.003)
Share Ecclesiastical States					0.0532***	0.0524***
					(0.009)	(0.009)
Battles					0.426	0.427
					(0.570)	(0.571)
Caloric Suitability (Pre-1500)						0.0000
						(0.001)
500 km Grid Fixed Effects	No	Yes	Yes	Yes	Yes	Yes
Observations	385	385	385	385	385	385
R^2	0.005	0.301	0.306	0.331	0.401	0.403

Notes. Robust Standard errors are reported in parentheses. Coefficient is statistically different from zero at the ***1 %, **5 % and *10 % level. The unit of observation is a grid cell of 2,500 km^2 size. All regressions include a constant not reported as well as seven 250,000 km^2 grid cell fixed effects each of them being equal to one if one of the 2,500 km^2 is located within the respective 250,000 km^2 grid cell.

European Historical Economics Society

EHES Working Paper Series

Recent EHES Working Papers

2016

EHES.100 Danger to the Old Lady of Threadneedle Street? The Bank Restriction Act and the regime shift to paper money, 1797-1821
Patrick K. O'Brien and Nuno Palma

EHES.99 The Role of human capital in pre-industrial societies: skills and earnings in eighteenth-century Castile (Spain)
Begoña Álvarez and Fernando Ramos Palencia

EHES.98 The Gross Agricultural Output of Portugal: A Quantitative, Unified Perspective, 1500-1850
Jaime Reis

EHES.97 The revealed comparative advantages of late-Victorian Britain
Brian D. Varian

EHES.96 Knowledge Shocks Diffusion and the Resilience of Regional Inequality
Alexandra López-Cermeño

EHES.95 Comparing Income and Wealth Inequality in Pre-Industrial Economies: Lessons from 18th-Century Spain
Esteban A. Nicolini and Fernando Ramos Palencia

EHES.94 Reconstruction of annual money supply over the long run: The case of England, 1279-1870
Nuno Palma

EHES.93 World trade, 1800-1938: a new data-set
Giovanni Federico and Antonio Tena-Junguito

All papers may be downloaded free of charge from: www.ehes.org
The European Historical Economics Society is concerned with advancing education in European economic history through study of European economies and economic history. The society is registered with the Charity Commissioners of England and Wales number: 1052680